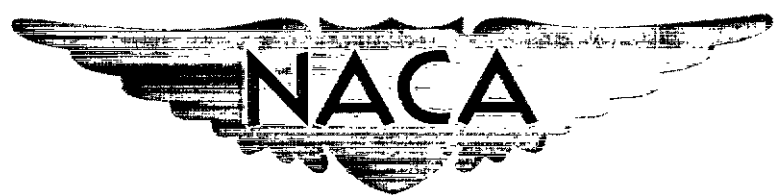


CONFIDENTIAL

Copy  
RM L56F15



# RESEARCH MEMORANDUM

INVESTIGATION OF SPOILER-SLOT-DEFLECTOR AILERONS AND OTHER  
SPOILER AILERONS ON A 45° SWEEPBACK-WING—FUSELAGE

COMBINATION AT MACH NUMBERS FROM 0.60 TO 1.03

By <sup>filed</sup> F. E. West, Jr., Charles F. Whitcomb,  
and James W. Schmeer

Langley Aeronautical Laboratory  
CLASSIFICATION ~~CHANGED~~  
Langley Field, Va.

To UNCLASSIFIED

By authority of NACA Rea also  
ARN-128 effective June 24, 1958  
AMT 9-9-58  
CLASSIFIED DOCUMENT

This material contains information affecting the National Defense of the United States within the meaning of the espionage laws, Title 18, U.S.C., Secs. 793 and 794, the transmission or revelation of which in any manner to an unauthorized person is prohibited by law.

## NATIONAL ADVISORY COMMITTEE FOR AERONAUTICS

WASHINGTON

September 11, 1956

RECEIVED

SEP 20 1956

CONFIDENTIAL

LANGLEY AERONAUTICAL LABORATORY

NACA RM L56F15



## NATIONAL ADVISORY COMMITTEE FOR AERONAUTICS

## RESEARCH MEMORANDUM

## INVESTIGATION OF SPOILER-SLOT-DEFLECTOR AILERONS AND OTHER

SPOILER AILERONS ON A  $45^\circ$  SWEEPBACK-WING-FUSELAGE

## COMBINATION AT MACH NUMBERS FROM 0.60 TO 1.03

By F. E. West, Jr., Charles F. Whitcomb,  
and James W. Schmeer

## SUMMARY

An investigation was conducted in the Langley 16-foot transonic tunnel to determine the characteristics of several flap-type spoiler ailerons, lower-surface deflector ailerons, and spoiler-slot-deflector ailerons. These controls were located in the vicinity of the 70-percent wing chord line and extended outboard to 87 percent of the wing semispan. The flap-type spoilers were tested at only one projection. The wing of the wing-body combination used in these tests had  $45^\circ$  sweepback, an aspect ratio of 4.0, a taper ratio of 0.60, and NACA 65A006 airfoil sections parallel to the plane of symmetry. Six-component force and moment data were obtained at Mach numbers from 0.60 to 1.03 (Reynolds numbers from  $5.05 \times 10^6$  to  $6.0 \times 10^6$ ) for an angle-of-attack range from  $0^\circ$  to approximately  $20^\circ$ .

The results show that, although the flap-type spoiler ailerons had more rolling-moment effectiveness than the spoiler-slot-deflector controls at low angles of attack, these ailerons became ineffective at high angles; whereas the latter control maintained appreciable effectiveness through the angle-of-attack range at all test Mach numbers. Removal of small inboard segments of the flap-type spoiler had little effect on the rolling-moment characteristics. Little or no improvement in the rolling-moment characteristics of a spoiler-slot-deflector control were obtained by either increasing the deflector chord length or by adding leading-edge chord-extensions to the outboard sections of the wing. The reversal of rolling-moment effectiveness at moderate angles of attack shown by deflector controls was not prevented either by decreasing deflector projection or by adding a gap between the deflector and the wing.

## INTRODUCTION

Flap-type spoiler ailerons and spoiler-slot-deflector ailerons are of interest for high-speed thin-wing configurations primarily because they require only small wing thicknesses and produce small torsional loads on wings. Spoiler-slot-deflector ailerons are of particular interest because these ailerons can provide fairly large rolling moments at high lift conditions. (For example, see refs. 1 and 2.) Such ailerons may also be designed to require less control force than flap-type spoiler ailerons.

However, there is a lack of data for these types of controls. In order to alleviate the lack of these data at transonic speeds, tests have been made in the Langley 16-foot transonic tunnel on a  $45^\circ$  sweptback-wing-body combination. This same model was also used for an investigation of retractable and plug spoiler ailerons. (See refs. 3 and 4.) The flap-type spoiler aileron and spoiler-slot-deflector ailerons used in the present tests were located in the vicinity of the 70-percent wing chord line and extended from the vicinity of the body to 87 percent of the semispan (same as the spoiler ailerons of refs. 3 and 4). The flap-type spoiler aileron, which had a fixed projection, was investigated with portions of the inboard sections removed and in combination with the wing slot. Two deflector chord lengths were used for the spoiler-slot-deflector ailerons, which utilized the previously mentioned spoiler and wing slot. One of the spoiler-slot-deflector ailerons was also investigated with outboard leading-edge chord-extensions added to the wing.

A deflector aileron with and without a gap between its trailing edge and the wing was also investigated at several projections.

Since spoiler ailerons are sometimes perforated to alleviate buffeting, a perforated plug spoiler aileron similar to one tested in reference 3, except for the perforations, was also investigated.

Force, moment, and pressure data were obtained through an angle-of-attack range at  $0^\circ$  sideslip for Mach numbers from 0.60 to 1.03. Reynolds number was about  $6 \times 10^6$ . The results of the six-component force and moment tests are presented in this paper.

## SYMBOLS

The forces are referenced to the wind axes and the moments are referenced to the body axes. These systems have their origin at a point in the plane of symmetry which corresponds to the 25-percent-chord station of the mean aerodynamic chord.

b	wing span
b <sub>i</sub>	inboard-end location of various controls
c	local basic wing chord (parallel to plane of symmetry)
c'	basic wing mean aerodynamic chord (parallel to plane of symmetry)
C <sub>D</sub>	drag coefficient, $\frac{\text{Drag}}{qS}$
C <sub>L</sub>	lift coefficient, $\frac{\text{Lift}}{qS}$
C <sub>l</sub>	rolling-moment coefficient produced by control, $\frac{\text{Rolling moment}}{qSb}$
C <sub>m, \delta c'</sub>	pitching-moment coefficient, $\frac{\text{Pitching moment}}{qSc'}$
C <sub>n</sub>	yawing-moment coefficient produced by control, $\frac{\text{Yawing moment}}{qSb}$
C <sub>y</sub>	lateral-force coefficient produced by control, $\frac{\text{Lateral force}}{qS}$
C <sub>Pb</sub>	base-pressure coefficient, $\frac{P_b - p}{q}$
M	free-stream Mach number
P <sub>b</sub>	static pressure at base of model
p	free-stream static pressure
q	free-stream dynamic pressure
S	total basic wing area
$\alpha$	angle of attack of fuselage center line, deg
$\delta_s$	projection of spoiler into airstream, fraction of c, measured perpendicular to wing chord line
$\delta_d$	projection of deflector into airstream, fraction of c, measured perpendicular to wing chord line
$\Delta C_D, \Delta C_L, \Delta C_m$	incremental coefficients produced by control

CONFIDENTIAL

## APPARATUS

## Tunnel and Model

The investigation was conducted in the Langley 16-foot transonic tunnel, the air flow and power characteristics of which are presented in reference 5.

With the exception of some very slight wing geometry changes, the wing-body combination used for these spoiler tests was the same as that used for the previous spoiler tests in the Langley 16-foot transonic tunnel. (See refs. 3 and 4.) Figure 1 presents the geometric details of the model. The steel wing had NACA 65A006 airfoil sections parallel to the plane of symmetry, sweep of quarter-chord line of  $45^\circ$ , taper ratio of 0.60, and aspect ratio of 4.0. It was constructed without incidence, dihedral, or twist and was mounted in a midwing position on the fuselage. The steel fuselage was a body of revolution with a fineness ratio of 10. The quarter-chord point of the wing mean aerodynamic chord was located at the longitudinal position of the maximum fuselage diameter.

## Lateral-Control and Chord-Extension Configurations

Table I shows some of the geometry of the lateral-control and chord-extension configurations used in the test program. More extensive geometric sectional details for one of the spoiler-slot-deflector ailerons and one of the deflector ailerons are shown in figures 1(b) and 1(c), respectively. All the devices were made of steel. The lateral controls were mounted only on the left wing.

Except for modifications involving the removal of small inboard segments, the same flap-type spoiler was used for all configurations that included a flap-type spoiler. This flap-type spoiler projected 7.8 percent of the local wing chord above the wing upper surface and extended along the 68.1-percent wing chord line. (See fig. 1(b).) When the inboard end of the spoiler extended to the fuselage ( $b_1 \approx 0.14b/2$ ), the juncture was sealed. The wing slot (3.8 percent of the wing chord) extended from 15- to 87-percent semispan station when used with other components extending into the body. The inboard end position was changed to 16 percent of the semispan when used with other components extending into 16 percent of the wing semispan. Ribs, which were parallel to the plane of symmetry, were located in the wing slot at 20-, 30-, 39-, 48-, 57-, 66-, 75-, and 83-percent semispan stations. These ribs had a height of 2.4 percent of the local wing chord and a width of 0.25 inch. Braces for the flap-type spoiler were mounted on top of these ribs (fig. 1(b)).

The deflectors of the spoiler-slot-deflector ailerons projected 4- and 5.5-percent of the local wing chord below the wing lower surface with the inboard end located at 16 percent of the semispan and at the fuselage, respectively. The change in deflector projection was obtained by changing deflector chord length. These deflectors were located along the 73.8-percent wing chord line and were fastened to the wing by seven braces (fig. 1(b)).

The deflector-alone configurations (see table I and fig. 1(c)) utilized a deflector that had a chord length of about 7.9 percent of the local wing chord when undeflected. (Note that chord length in terms of local wing chord changes with control projection.) Although this deflector extended inboard to the fuselage, it was not contoured to fit the fuselage closely and the juncture was not sealed. For the deflector configurations having a gap between the deflector and wing surface, spacers with a height of 2 percent of the local wing chord and a width of 5/16 inch were located at seven semispan stations. For one of the deflector-alone configurations, seven simulated brackets, which were perpendicular to the deflector hinge line, were distributed along the front face of the deflector and aligned with the spacers.

The perforated plug spoiler had vertical slots whose width and spacing were 0.5 percent of the local wing chord. The distance between the top edge of the slots and the top edge of the spoiler was the same as the slot width. This spoiler was similar to a solid spoiler of reference 3, with the exception of the perforations and a solid spoiler thickness of 0.015c compared with a perforated spoiler thickness of 0.008c.

The leading-edge chord-extensions, which are similar to those discussed in references 6 and 7, extended forward 15 percent of the local wing chord from the 65-percent semispan station to the wing tip. The chord-extensions had the same section ordinates back to their maximum thickness as did the basic airfoil sections at corresponding spanwise stations. Between the maximum thickness of the chord-extensions and the maximum thickness of the wing, the airfoil contour paralleled the wing chord line.

## TESTS

Data were obtained for the 17 configurations listed in table I. The configurations were generally tested through a maximum angle-of-attack range of  $0^\circ$  to approximately  $21.5^\circ$  for Mach numbers from 0.60 to 0.94 and up to maximum angles of  $19.4^\circ$ ,  $15.4^\circ$ , and  $13.2^\circ$  for Mach numbers of 0.98, 1.00, and 1.03, respectively. These maximum values were not attained for all of the configurations because of model stress or tunnel power limitations. The variation of Reynolds number based on the mean aerodynamic chord with Mach number is presented in figure 2.

## CORRECTIONS AND ACCURACIES

The measured lift and drag data were adjusted to a condition of free-stream static pressure at the base of the fuselage by using base pressures averaged from three static orifices spaced equidistantly around the base annulus just inside the base of the model. The variation of the faired mean base pressure for all configurations at constant Mach numbers with angle of attack is presented in figure 3. Generally, the values for the individual configurations did not deviate from these curves by more than  $\pm 0.015$  and never varied more than  $\pm 0.03$  (equivalent to a drag coefficient of  $\pm 0.0007$ ).

Inasmuch as the base pressures were adjusted to free-stream static-pressure conditions, only the sting interference effects on the flow conditions ahead of the model base remain to be considered. These sting interference effects are believed to be small and therefore were neglected. Furthermore, all lateral-control configuration changes were made on the wing which was remote from the sting; therefore the sting effects would be nearly constant for all of the configurations. The effects of tunnel-wall interference were small for the Mach number range of these tests and were neglected. (See ref. 8.)

The accuracy of the measured coefficients, based on balance accuracy and repeatability of data, is believed to be within the following limits:

$C_L$ . . . . .	$\pm 0.01$
$C_D$ at low angles of attack . . . . .	$\pm 0.001$
$C_D$ at highest angles of attack . . . . .	$\pm 0.005$
$C_m$ . . . . .	$\pm 0.005$
$C_l$ . . . . .	$\pm 0.001$
$C_n$ . . . . .	$\pm 0.001$
$C_y$ . . . . .	$\pm 0.002$

The angles of attack are estimated to be accurate to  $\pm 0.1^\circ$ .

## RESULTS AND DISCUSSION

Data showing the variation of the aerodynamic characteristics with angle of attack for the several tested configurations are presented in the figures listed in table I. The primary purpose of figure 4 is to show the data for the basic model with and without chord-extensions which were used as a basis to obtain the incremental changes due to the

various lateral controls. Basic model characteristics for a similar configuration have been discussed in reference 9. The effect of chord-extensions on the aerodynamic characteristics for a similar configuration has been discussed in references 6 and 7.

The figures for the lateral-control configurations (figs. 5 to 9 and 11) compare rolling-moment, yawing-moment, and lateral-force characteristics for various configurations as well as the incremental lift, drag, and pitching-moment characteristics resulting from the presence of the controls. Figure 10 shows the effect on rolling-moment and yawing-moment characteristics of adding a deflector to the opposite wing of a spoiler-slot-deflector aileron (synthesized data). A summary figure showing effects of Mach number on rolling-moment effectiveness for several configurations is presented in figure 12.

#### Characteristics of Various Flap-Type Spoilers and Spoiler-Slot-Deflector Configurations

Flap-type spoiler effectiveness.- The rolling-moment effectiveness shown in figure 5(a) for the flap-type spoiler ailerons varied in much the same manner with angle of attack as did the retractable and plug spoiler effectiveness presented in reference 3 for a similar model and spoiler span and wing location. The large decreases in rolling-moment coefficient for these controls at the higher angles of attack result from flow separation on the wing. (See ref. 4.) Although the flap-type spoiler ailerons produced larger rolling-moment coefficients at low angles of attack than the retractable or plug spoiler ailerons of references 3 and 4, the gains were relatively smaller than the increase in control projection (0.04c to 0.078c). The lack of proportionality probably occurred mainly because of differences in spoiler-aileron profile. (See ref. 10.) However, nonlinear variations of rolling-moment coefficient with control projection also could have had an effect on the comparative values.

Reference 4 indicated that large negative pressures behind the inboard-spoiler sections on a similar basic model caused the inboard sections to be ineffective in providing rolling moment and to contribute heavily to drag. Therefore, it appeared reasonable that cutting the inboard end of a spoiler away from the body might result in no appreciable effect on rolling moment and a decrease in drag. Figure 5(a) shows that the inboard-end location of the flap-type spoiler can be moved from the body ( $b_1 \approx 0.14b/2$ ) to  $0.16b/2$  without resulting in rolling-moment losses. However, further movement to  $0.22b/2$  usually resulted in slight decreases in rolling moment. The effects on the drag increments are discussed briefly in a subsequent section.



Spoiler-slot-deflector effectiveness.- Figure 6(a) shows that the addition of the wing slot immediately behind the spoiler with the inboard end at the  $0.16b/2$  wing station generally produced some increase in the rolling-moment effectiveness of the control throughout the angle-of-attack and Mach number ranges tested. The same figure shows that the further addition of the  $0.04c$  projected lower-surface deflector to the control configuration provided a large improvement at the high angles for all test Mach numbers. Similar results were obtained from the transonic straight wing investigation of reference 2. Thus, loss of control effectiveness that occurred for the spoiler-slot configuration at the highest test angles was eliminated by addition of the deflector. Unfortunately, the addition of the deflector reduced the effectiveness at low angles of attack throughout the Mach number range. These reductions at low angles are attributed to the deflector acting as a lower-surface spoiler; that is, the deflector caused pressure increases on the wing lower surface. The magnitude of these reductions increased considerably when the deflector projection was increased from  $0.04c$  to  $0.0550c$ . (See fig. 7(a).) Figure 7(a) also shows that the increase in deflector projection did not provide the anticipated increase in effectiveness of the control at high angles of attack. The control with the longer deflector projection had its inboard end at the body ( $b_1 \approx 0.14b/2$ ) instead of at the position of  $0.16b/2$  for the control with the shorter deflector. Based on the results of figure 5(a), it is believed that the effect of this small geometric difference is negligible. The trend of the results for the two spoiler-slot-deflector ailerons indicate that a deflector of shorter chord length than the shortest one tested may be desirable.

Basically, it is believed that the major effects of adding a deflector to a spoiler-slot control are to increase the lower surface pressures ahead of the deflector and to reduce these pressures behind the deflector. In order for a deflector to improve the control effectiveness, the second effect should be larger than the first effect throughout the angle-of-attack range. Apparently, the deflectors of the present investigation did not satisfy these requirements at low angles of attack. At high angles of attack, the deflectors were satisfactory primarily because flow separation probably occurred between the deflector and wing trailing edge over most of the control span. The occurrence of this flow separation would greatly reduce the large trailing-edge lift load normally carried by the wing at high angles of attack. (See fig. 14 in ref. 4.)

Mach number effects.- The effects of Mach number on the rolling-moment coefficients for several of the spoiler configurations are shown in figure 12. Inasmuch as these effects were similar with and without a slot behind the flap-type spoiler aileron, results for the spoiler-slot configuration are not shown. At  $0^\circ$  angle of attack, the rolling-moment coefficients for the flap-type spoiler aileron increased slightly with increasing Mach numbers up to near-sonic speeds. However, the opposite trend occurred for the spoiler-slot-deflector configurations at low

angles of attack. A change in deflector projection changed the values of  $C_l$  but had little effect on the variation of  $C_l$  with Mach number. With increasing angle of attack, the trends with Mach number gradually become similar for all of the configurations. Also, with increasing angle of attack, the Mach number effects become larger, especially at the higher test Mach numbers.

Spoiler effectiveness with leading-edge chord-extensions.- Since devices such as leading-edge chord-extensions are often necessary on swept wings for improving the longitudinal stability characteristics, the effects of these devices on lateral-control effectiveness are of interest. Such devices would be expected to be effective in improving lateral-control effectiveness in the same angle-of-attack range where they cause improvements in longitudinal stability. (See fig. 4(c).) Reference 11 fulfills this expectation by showing that the addition of chord-extensions and a full-span leading-edge flap to a swept-wing model resulted in considerable improvements in the effectiveness of a spoiler-slot-deflector aileron. The leading-edge flap was drooped  $6^\circ$  with respect to the wing chord line about the 20-percent chord line. The basic model was similar to the model of the present tests except the wing taper ratio was 0.3 instead of 0.6. However, as shown in figure 7(a), adding chord-extensions to the model of the present tests caused little or no improvement in the effectiveness of one of the spoiler-slot-deflector ailerons. There were also adverse effects, as in the investigation of reference 11, at the higher angles of attack where leading-edge modifications have no effect on longitudinal-stability characteristics.

Yawing-moment coefficient.- Figure 5(b) shows that the flap-type spoiler aileron produced favorable but large yawing-moment coefficients over the model test angle-of-attack range up to  $8^\circ$ . Above this angle range, the yawing-moment coefficients decreased rapidly at all Mach numbers and became adverse at some of the Mach numbers. Removing the two different length inboard sections of the spoiler had no significant effect on the yawing-moment coefficients.

Figure 6(b) shows that the effect of adding a wing slot immediately behind a spoiler was to make the yawing moments less favorable in the high angle-of-attack range. With the further addition of the 0.04c-projected deflector to the spoiler-slot configuration, the yawing moments were appreciably increased over the entire angle and Mach number ranges. The reversals in yawing moment in the higher angle range were eliminated within the range of the investigation.

Increasing the deflector projection from 0.04c to 0.055c increased the yawing moments slightly over the low angle range for all the Mach numbers tested but had no significant or consistent effect at the higher angles. (See fig. 7(b).) This effect in the low angle range was

opposite to the effect the change in deflector chord length had on rolling-moment coefficient.

Figure 7(b) shows that addition of chord-extensions to one of the spoiler-slot-deflector configurations resulted in slightly increased yawing moments at moderate angles of attack. This change had also caused increased rolling moments at moderate angles of attack. However, the configuration change did not result in a decrease in yawing-moment coefficient at high angles as it generally did in the case of rolling-moment coefficient.

Lateral-force coefficient.- The trend of lateral-force coefficient for all of the spoiler-aileron configurations (see figs. 5(c), 6(c), 7(c)) was to decrease with increasing angle of attack.

Incremental lift, drag, and pitching-moment coefficients.- The increments of lift, drag, and pitching-moment coefficients for the various flap-type spoiler and spoiler-slot-deflector configurations are presented in parts (d), (e), and (f) of figures 5, 6, and 7. The overall trends of these increments with increasing angle of attack are similar to trends established for other spoiler ailerons in previous papers. (For example, see ref. 3.)

The apparent lack of correlation between the relative magnitudes of  $C_l$  and  $\Delta C_L$  for the various configuration changes (compare parts (a) with (d) for figures 5, 6, and 7) means, of course, that some of the changes in geometry had appreciable effects on the lateral location of the center of load.

As stated previously, removal of small inboard segments of the spoiler ailerons was done primarily to reduce drag without incurring significant reductions in rolling-moment effectiveness. Figure 5(e) shows that moving the inboard end of the spoiler from the fuselage ( $b_1 \approx 0.14b/2$ ) to  $0.16b/2$  had no significant effects. Further removal of inboard segments to  $0.22b/2$  resulted in drag reductions at Mach numbers of 0.94 and above. At subsonic speeds, as indicated at  $M = 0.60$ , removal of inboard segments had some adverse effects on drag.

#### Characteristics for Various Deflector Configurations

One of the problems often associated with spoiler-aileron controls is that the yawing moments, although favorable, are higher than desirable. One method of reducing the yawing moments due to a spoiler-slot-deflector aileron would be to project the deflector part of the control on one wing panel simultaneously with projection of the complete control on the

opposite wing panel. A shortcoming in this solution, however, is the fact that lower-surface devices such as spoilers or deflectors suffer reversals in rolling-moment effectiveness at moderately high angles of attack. (See ref. 3.)

In an attempt to avoid these reversals, an investigation was made of the effects of decreasing deflector projection and of leaving a gap between the deflector trailing edge and the wing surface. As shown in figures 8(a) and 9(a), however, all of the deflector configurations tested underwent a rolling-moment reversal at the higher angles of attack.

The rolling- and yawing-moment coefficients that would result (neglecting any carryover effects) from simultaneous deflection of the spoiler-slot-0.055c deflector aileron and a deflector aileron ( $\delta_d = 0.045c$ , no gap) on opposite wing panels are shown in figure 10. These synthesized data indicate the beneficial effects of the deflector aileron on both rolling moments and yawing moments up to angles of attack of about  $10^\circ$  to  $12^\circ$ . At higher angles of attack, however, the effects are detrimental.

One of the deflector ailerons ( $\delta_d = 0.05c$ , 0.02c gap) was tested with seven simulated brackets mounted on the front face of the deflector and in line with the braces. The results, shown in figure 9, indicate no significant differences due to the addition of the brackets.

## Effect on the Aerodynamic Characteristics of

### Perforating a Plug Spoiler

As spoiler ailerons are often perforated to alleviate buffet problems, aerodynamic data for perforated spoiler-aileron configurations are of interest. The results of the present tests using a perforated plug spoiler are compared in figure 11 with results from the similar solid spoiler test reported in reference 3. Here, it is shown, that perforating the spoiler generally caused slight reductions in rolling-moment, yawing-moment, and incremental drag coefficients. Somewhat similar effects of perforating are shown in reference 12.

## CONCLUSIONS

An investigation was conducted with inboard flap-type spoiler ailerons, deflector ailerons, and spoiler-slot-deflector ailerons mounted on a  $45^\circ$  sweptback-wing-fuselage combination. These controls were located in the vicinity of the 70-percent wing chord line and extended outboard to 87 percent of the wing semispan. Six-component force and moment data were obtained at Mach numbers from 0.60 to 1.03 (Reynolds numbers from

$5.05 \times 10^6$  to  $6.0 \times 10^6$ ) for an angle-of-attack range from  $0^\circ$  to about  $20^\circ$ . The results indicate the following conclusions:

- ✓ 1. Flap-type spoiler ailerons were generally more effective than the spoiler-slot-deflector controls at low angles of attack; however, at high angles of attack the spoiler aileron became ineffective, whereas the spoiler-slot-deflector controls maintained appreciable rolling-moment effectiveness at all test Mach numbers.
2. Removal of small inboard segments (8 percent of the wing semi-span or less) of the flap-type spoiler aileron had little or no effect on rolling-moment effectiveness and had a favorable effect on drag at the higher Mach numbers.
3. Increasing the chord of the deflector (so that projection into the airstream increased from 4 percent to 5.5 percent of the wing chord) reduced the rolling-moment effectiveness of the spoiler-slot-deflector control at low angles of attack and had no beneficial effects at the higher angles.
4. Adding outboard leading-edge chord-extensions to the wing had slight beneficial effects at moderate angles of attack and detrimental effects at higher angles of attack on the rolling-moment effectiveness of a spoiler-slot-deflector aileron.
5. Decreasing deflector-aileron projection or adding a gap between the deflector aileron and the wing lower surface did not prevent reversals in rolling-moment effectiveness which occurred at moderate angles of attack.

Langley Aeronautical Laboratory,  
National Advisory Committee for Aeronautics,  
Langley Field, Va., May 25, 1956.

## REFERENCES

1. Vogler, Raymond D.: Wind-Tunnel Investigation at High Subsonic Speeds of a Spoiler-Slot-Deflector Combination on an NACA 65A006 Wing With Quarter-Chord Line Swept Back  $32.6^{\circ}$ . NACA RM L53D17, 1953.
2. Vogler, Raymond D.: Wind-Tunnel Investigation at Transonic Speeds of a Spoiler-Slot-Deflector Combination on an Unswept NACA 65A006 Wing. NACA RM L53J21, 1953.
3. West, F. E., Jr., Solomon, William, and Brummal, Edward M.: Investigation of Spoiler Ailerons With and Without a Gap Behind the Spoiler on a  $45^{\circ}$  Sweptback Wing-Fuselage Combination at Mach Numbers From 0.60 to 1.03. NACA RM L53G07a, 1953.
4. Hallissy, Joseph M., Jr., West, F. E., Jr., and Liner, George: Effects of Spoiler Ailerons on the Aerodynamic Load Distribution Over a  $45^{\circ}$  Sweptback Wing at Mach Numbers From 0.60 to 1.03. NACA RM L54C17a, 1954.
5. Ward, Vernon G., Whitcomb, Charles F., and Pearson, Merwin D.: Air-Flow and Power Characteristics of the Langley 16-Foot Transonic Tunnel With Slotted Test Section. NACA RM L52E01, 1952.
6. West, F. E., Jr., Liner, George, and Martz, Gladys S.: Effect of Leading-Edge Chord-Extensions on the Aerodynamic Characteristics of a  $45^{\circ}$  Sweptback Wing-Fuselage Combination at Mach Numbers of 0.40 to 1.03. NACA RM L53B02, 1953.
7. West, F. E., Jr., and Henderson, James H.: Relationship of Flow Over a  $45^{\circ}$  Sweptback Wing With and Without Leading-Edge Chord-Extensions to Longitudinal Stability Characteristics at Mach Numbers From 0.60 to 1.03. NACA RM L53H18b, 1953.
8. Whitcomb, Charles F., and Osborne, Robert S.: An Experimental Investigation of Boundary Interference on Force and Moment Characteristics of Lifting Models in the Langley 16- and 8-Foot Transonic Tunnels. NACA RM L52L29, 1953.
9. Hallissy, Joseph M., and Bowman, Donald R.: Transonic Characteristics of a  $45^{\circ}$  Sweptback Wing-Fuselage Combination. Effect of Longitudinal Wing Position and Division of Wing and Fuselage Forces and Moments. NACA RM L52K04, 1953.
10. Johnson, Harold S.: Wind-Tunnel Investigation at High Subsonic Speeds of the Effect of Spoiler Profile on the Lateral Control Characteristics of a Wing-Fuselage Combination With Quarter-Chord Line Swept Back  $32.6^{\circ}$  and NACA 65A006 Airfoil Section. NACA RM L53J05a, 1953.

11. Thompson, Robert F., and Taylor, Robert T.: Effect of a Wing Leading-Edge Flap and Chord-Extension on the High Subsonic Control Characteristics of a Spoiler-Slot-Deflector Control Located at Two Spanwise Positions. NACA RM L54I09, 1954.
12. Vogler, Raymond D.: Wind-Tunnel Investigation at High Subsonic Speeds of Spoilers of Large Projection on an NACA 65A006 Wing With Quarter-Chord Line Swept Back  $32.6^\circ$ . NACA RM L51L10, 1952.

TABLE I.  
GEOMETRY OF TEST CONFIGURATIONS  
(Not to scale)

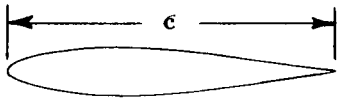

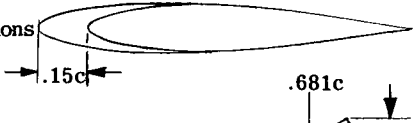
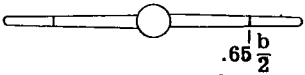
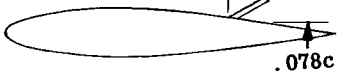

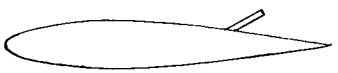
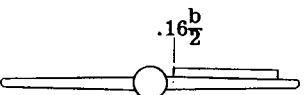
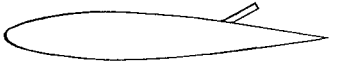
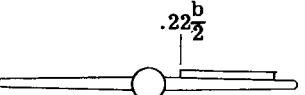
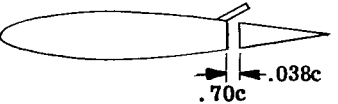
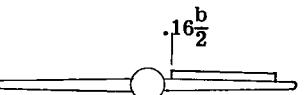
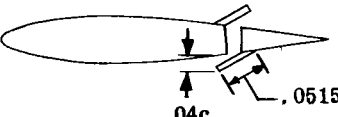
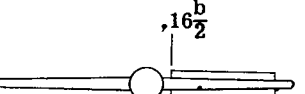
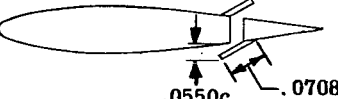
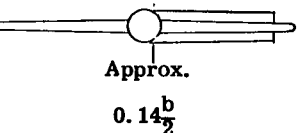
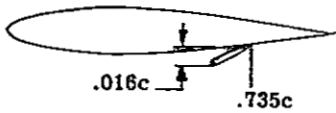
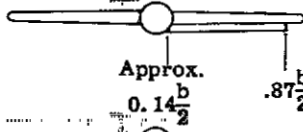
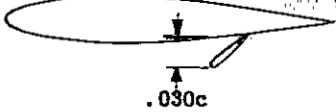

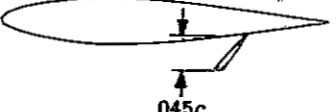

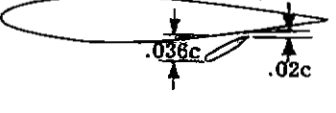

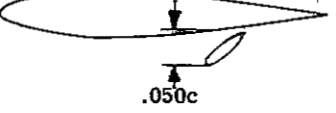

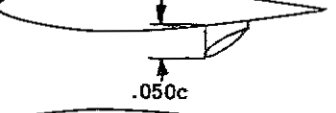

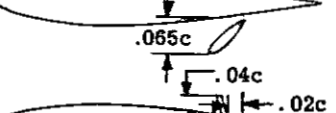

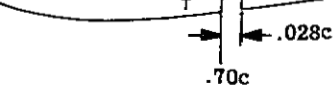
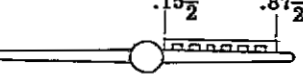
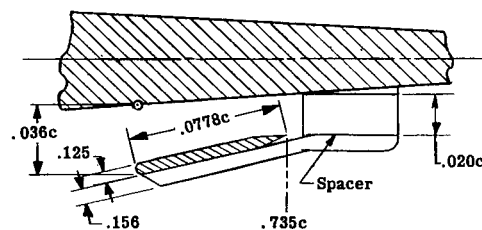
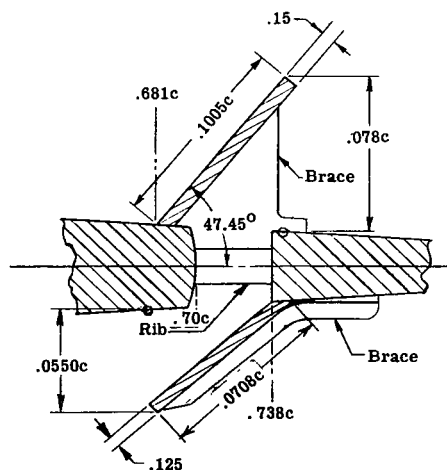
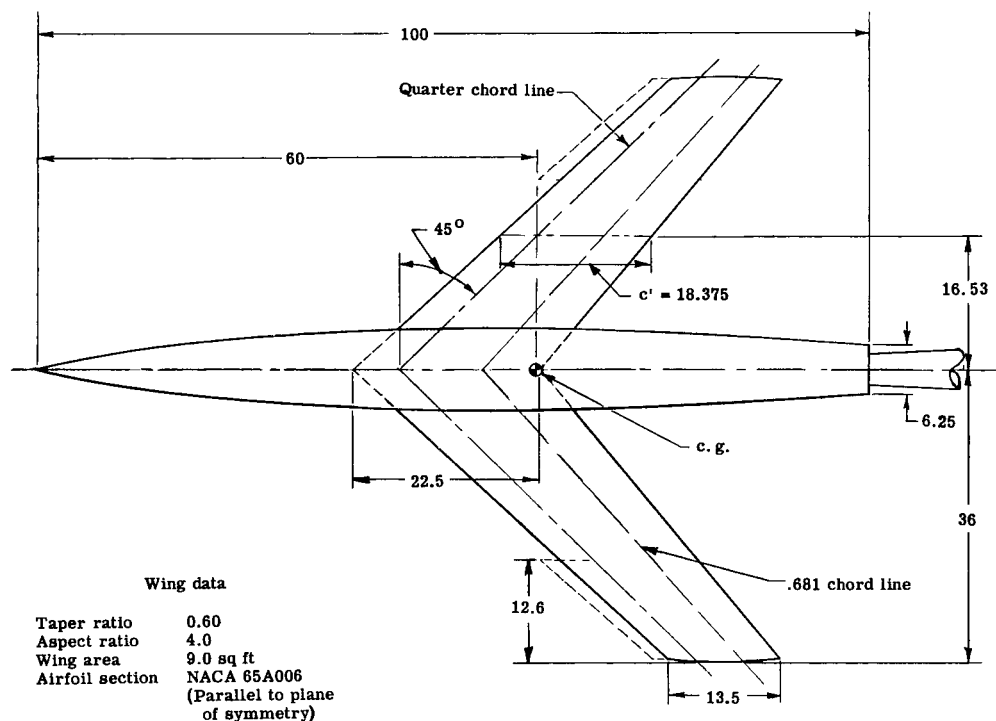
Configuration	Wing section view	Model front view	Figure number
Basic wing			4
L. E. chord-extensions			4
Flap spoiler			5
Flap spoiler			5,6
Flap spoiler			5
Flap spoiler-slot			6
Spoiler-slot-deflector			4,6,7
Spoiler-slot-deflector (with and without L. E. chord extensions)			7



TABLE I.- Concluded  
 GEOMETRY OF TEST CONFIGURATIONS  
 (Not to scale)

Configuration	Wing section view	Model front view	Figure number
Deflector			8
Deflector			8
Deflector			8
Deflector with gap			9
Deflector with gap			9
Deflector with gap and simulated brackets			9
Deflector with gap			9
Perforated plug-spoiler			11



(b) Spoiler-slot-deflector aileron.

(c) Deflector aileron.

Figure 1.- Diagram and dimensional details of wing-fuselage model and two different spoiler-control configurations. (All linear dimensions in inches except as noted.)

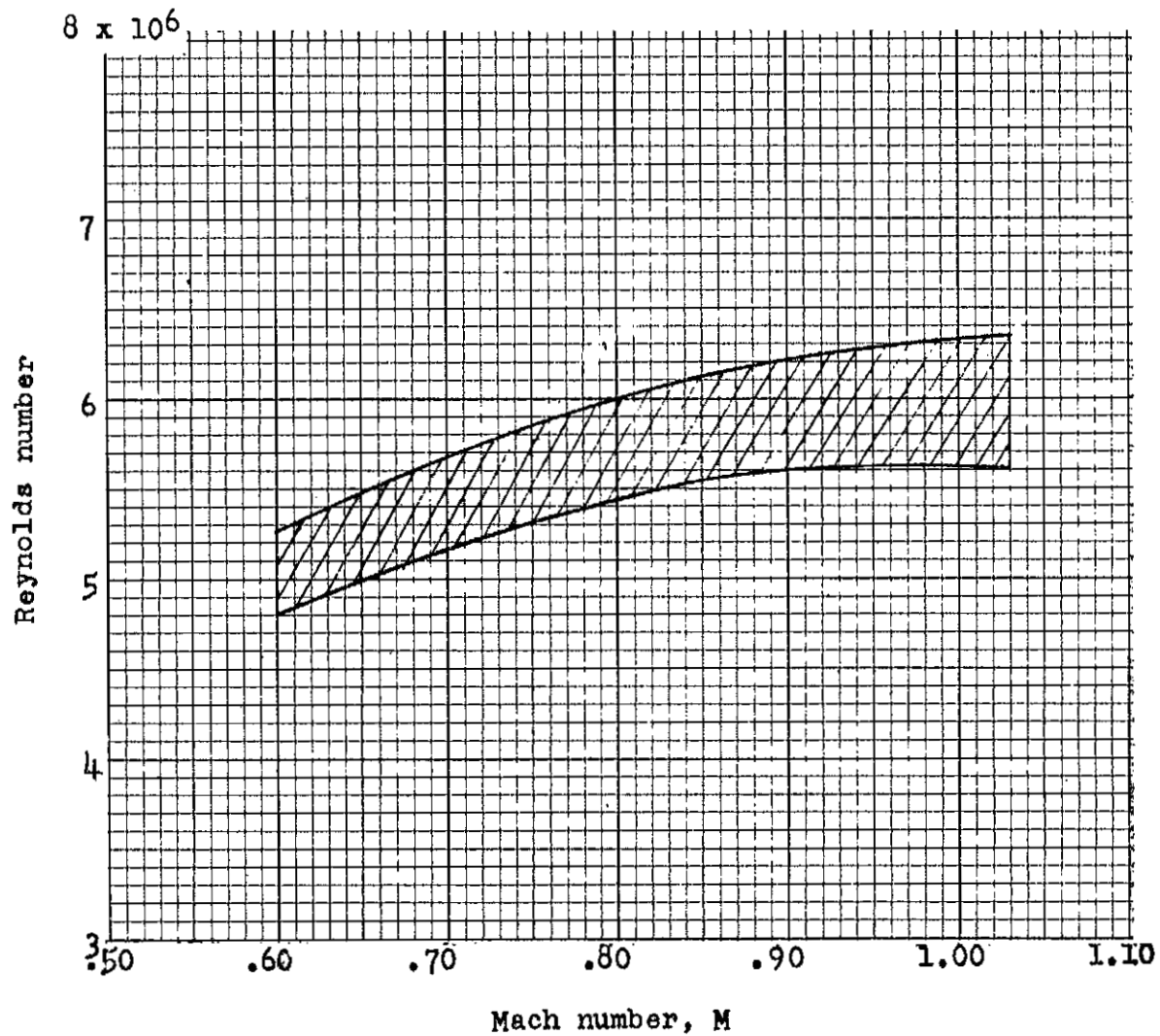


Figure 2.- Variation of Reynolds number (based on mean aerodynamic chord) with Mach number.

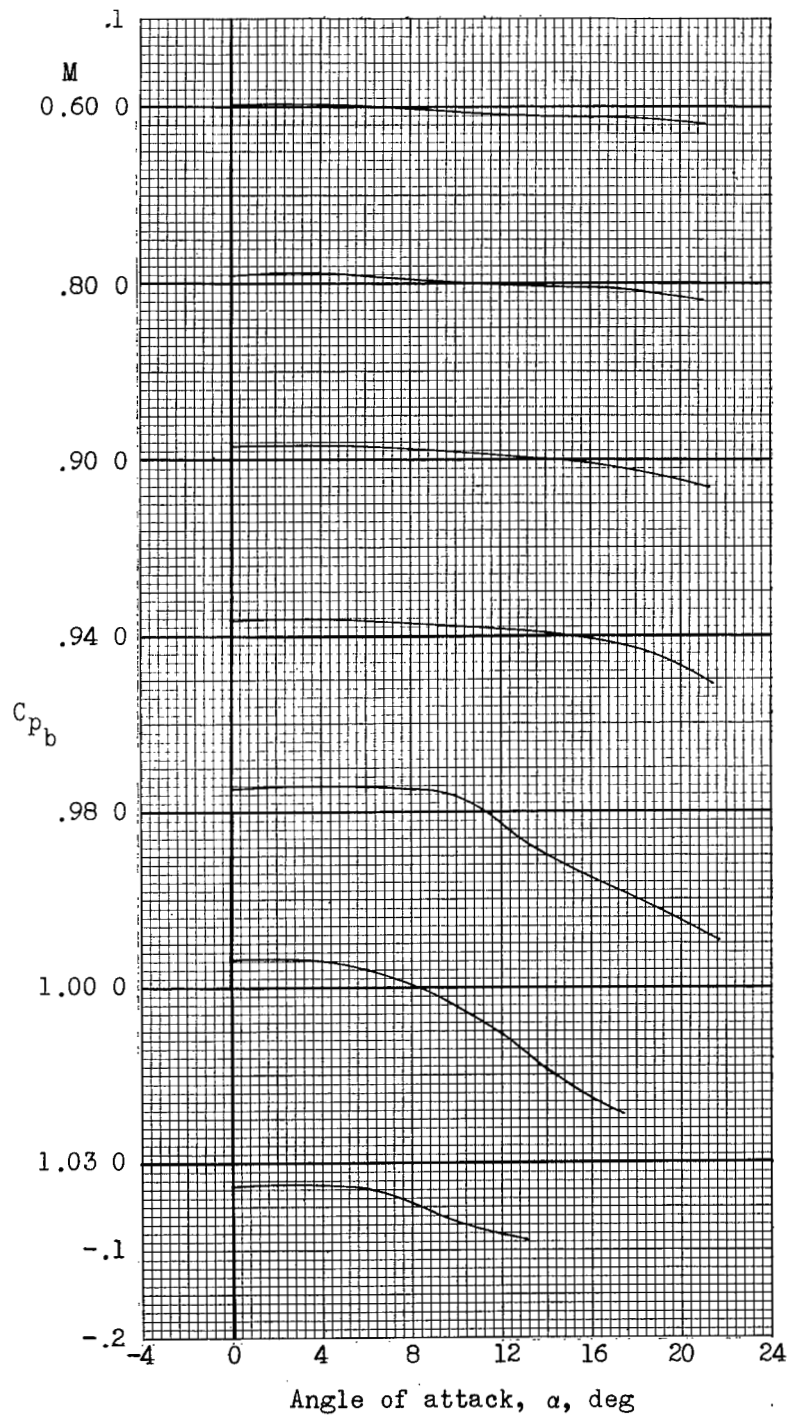
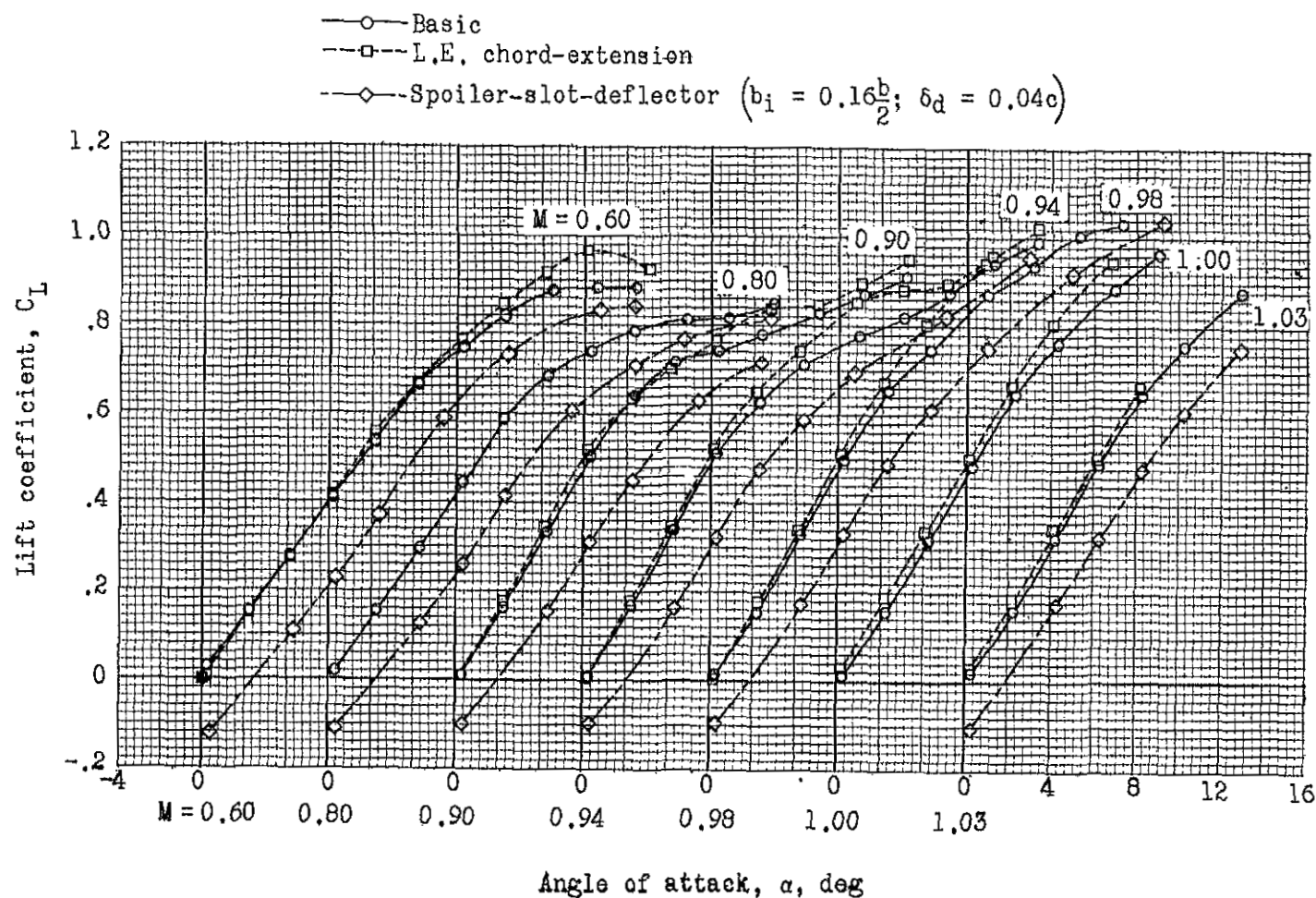
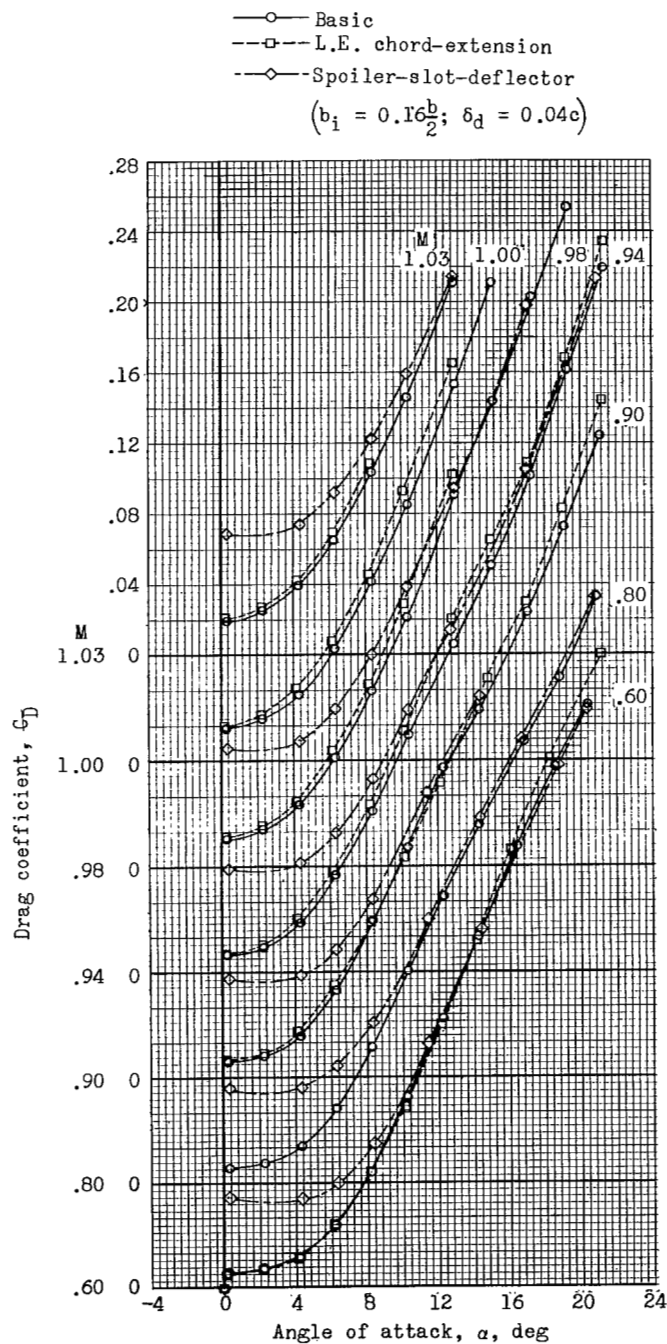


Figure 3.- Average base-pressure coefficient for all configurations.



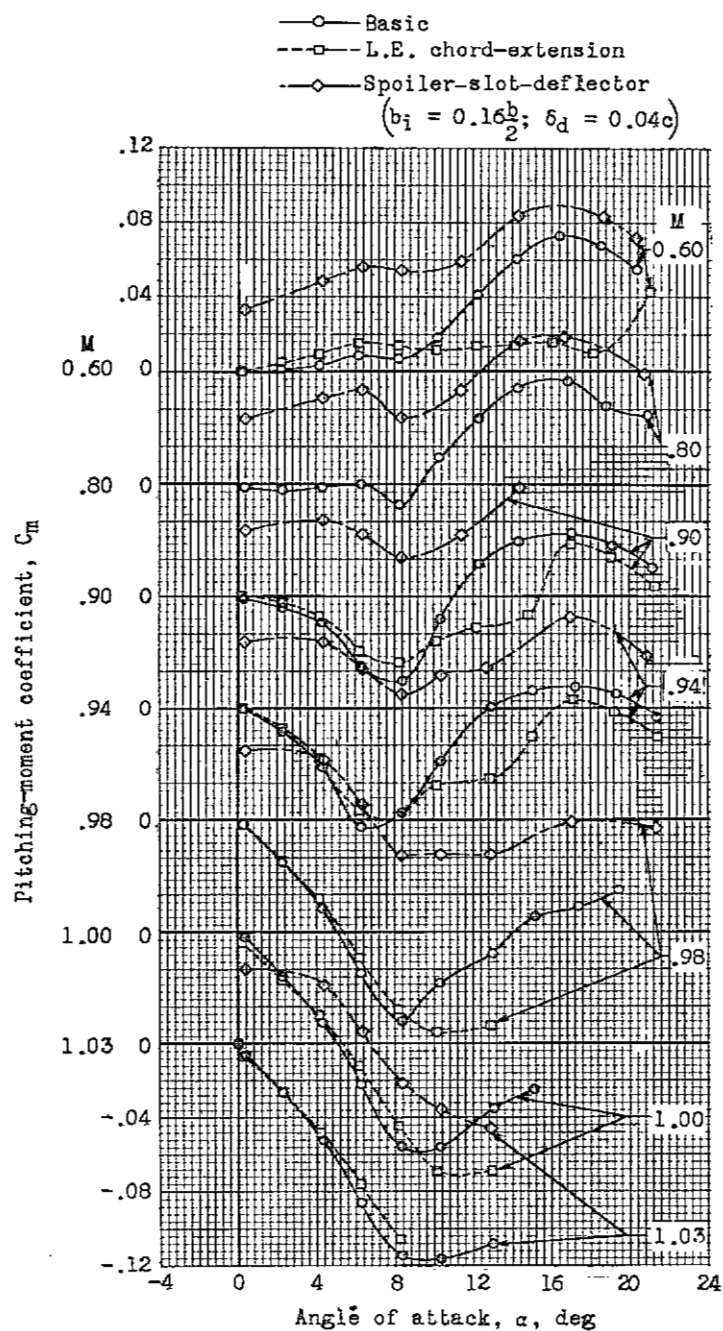
(a) Lift coefficient.

Figure 4.- Lift, drag, and pitching-moment characteristics for the basic and leading-edge chord-extension configurations and a spoiler-slot-deflector configuration.



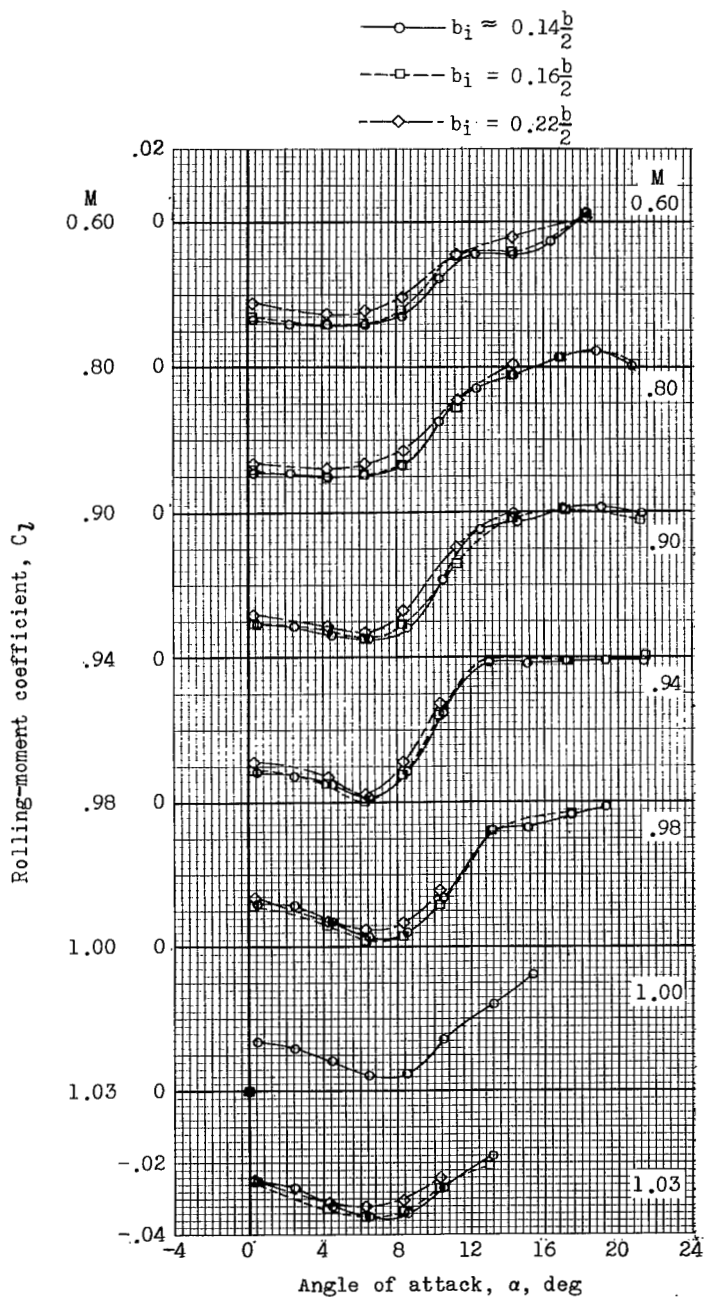
(b) Drag coefficient.

Figure 4.- Continued.



(c) Pitching-moment coefficient.

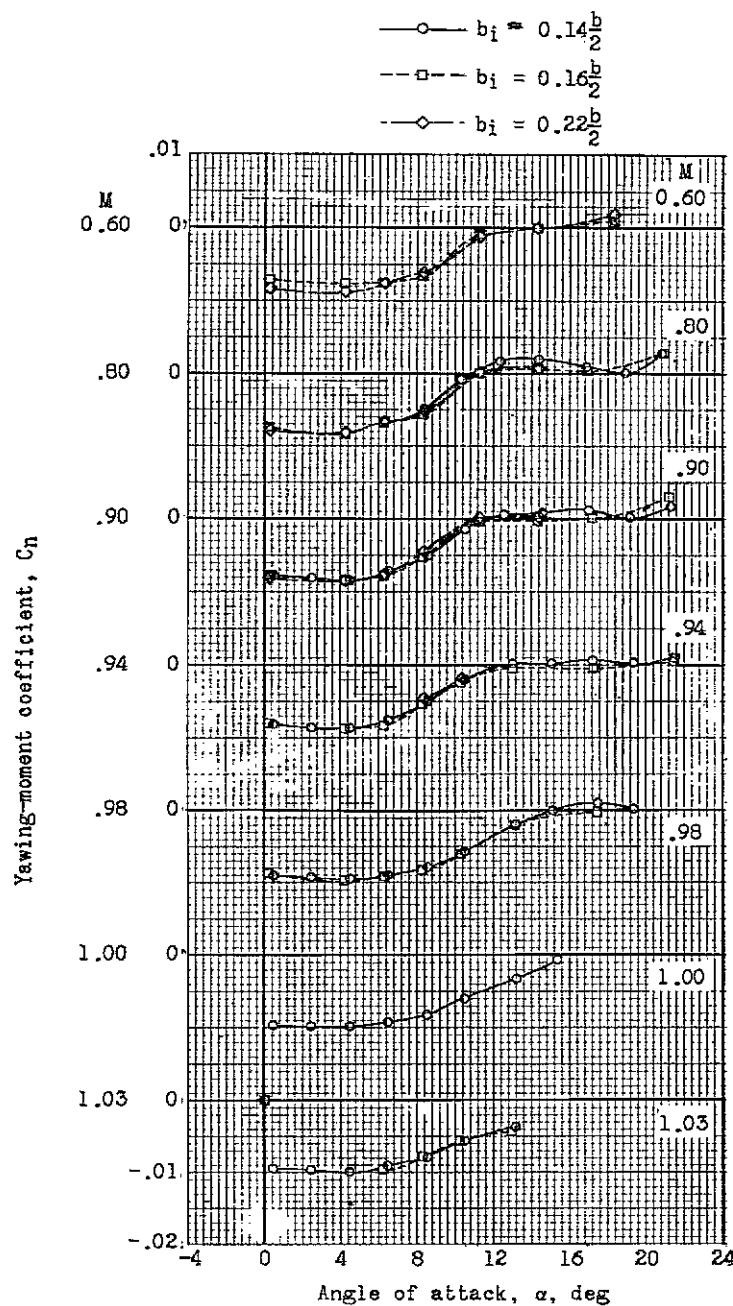
Figure 4.- Concluded.



(a) Rolling-moment coefficient.

Figure 5.- Aerodynamic characteristics of flap-type spoiler configurations showing the effect of varying spoiler inboard-end location.





(b) Yawing-moment coefficient.

Figure 5.- Continued.

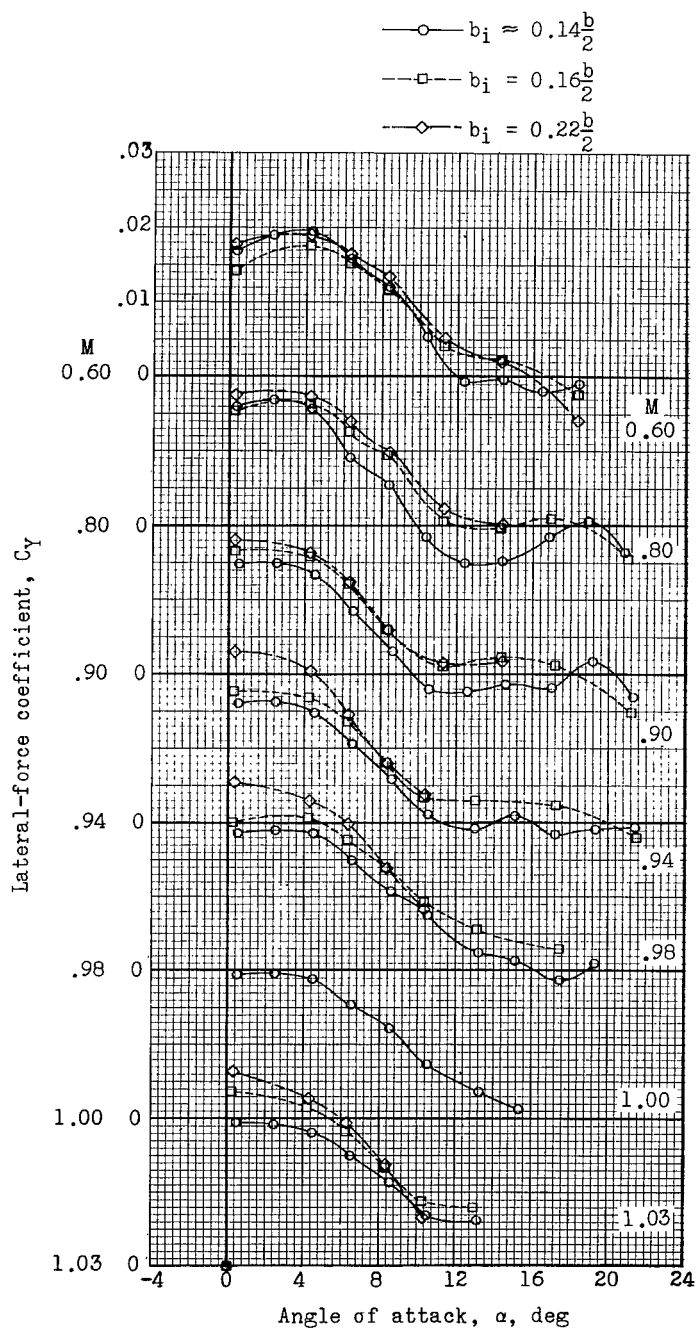
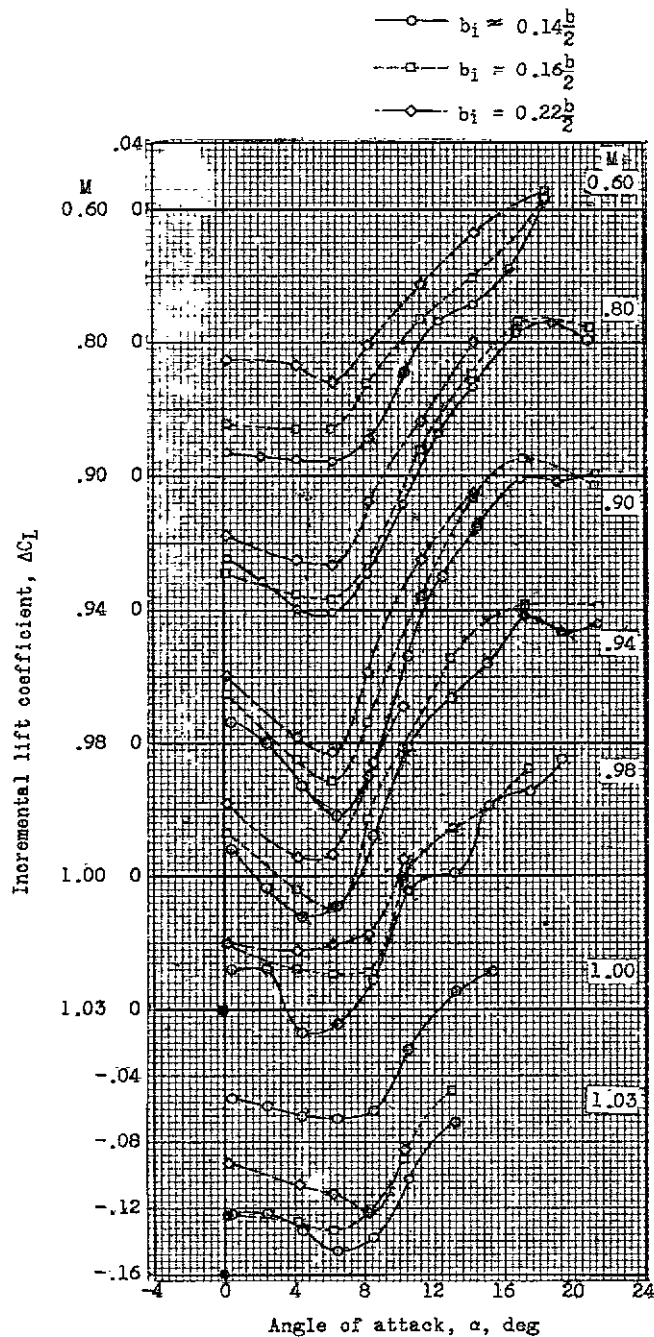
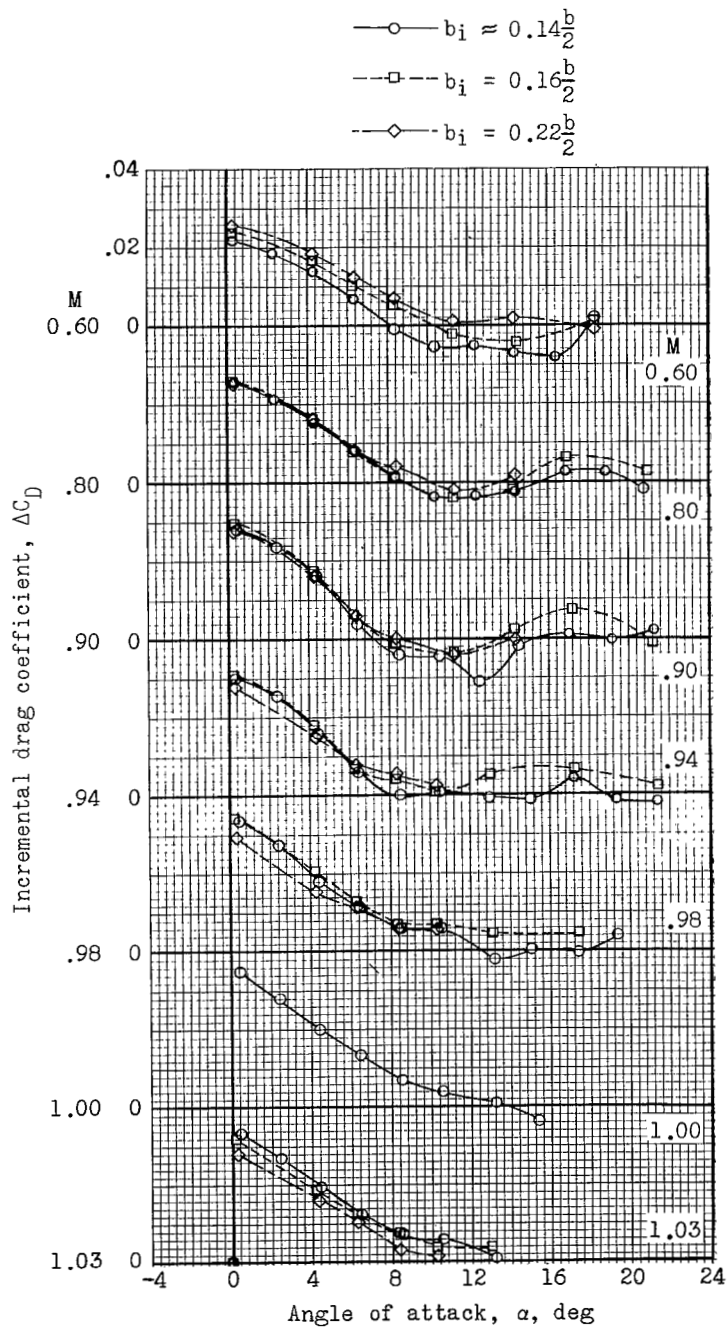


Figure 5.- Continued.



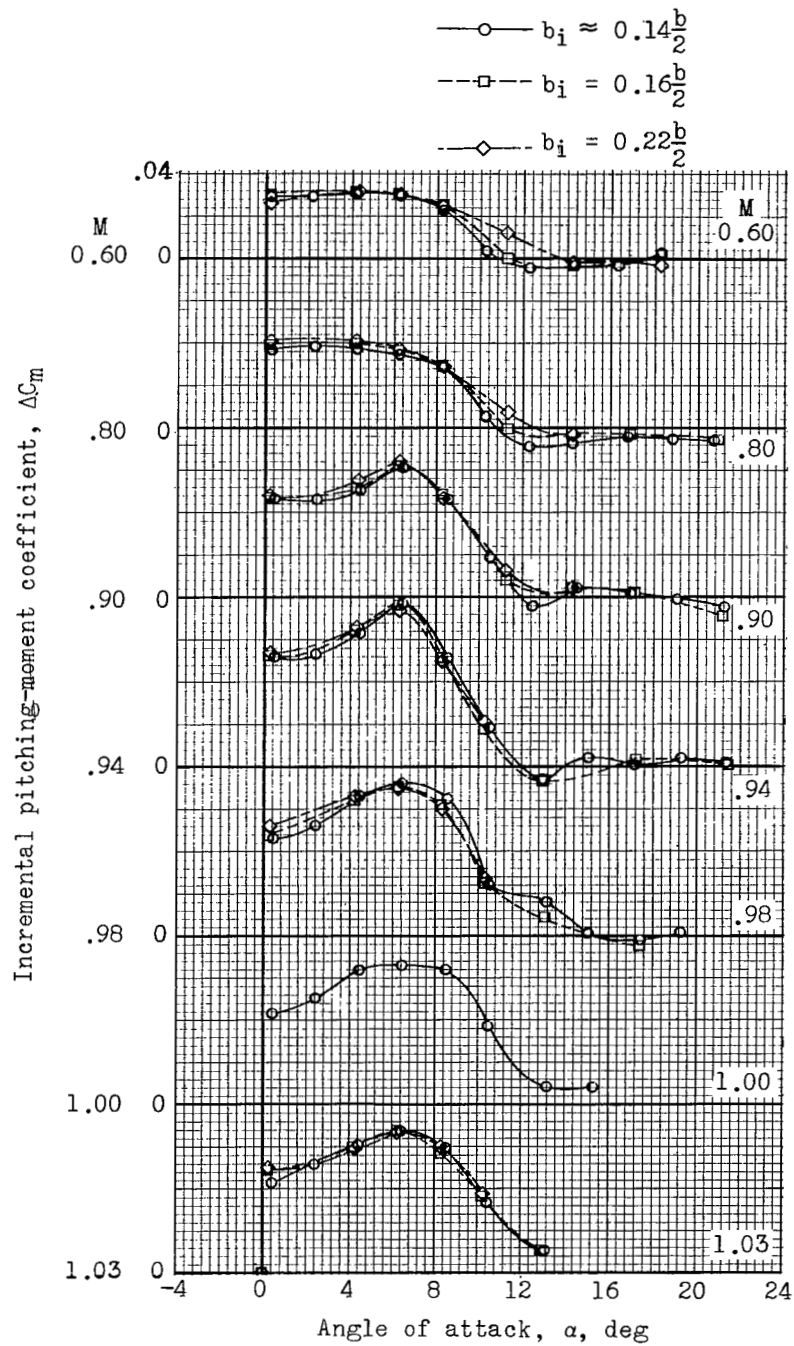
(d) Incremental lift coefficient.

Figure 5.- Continued.



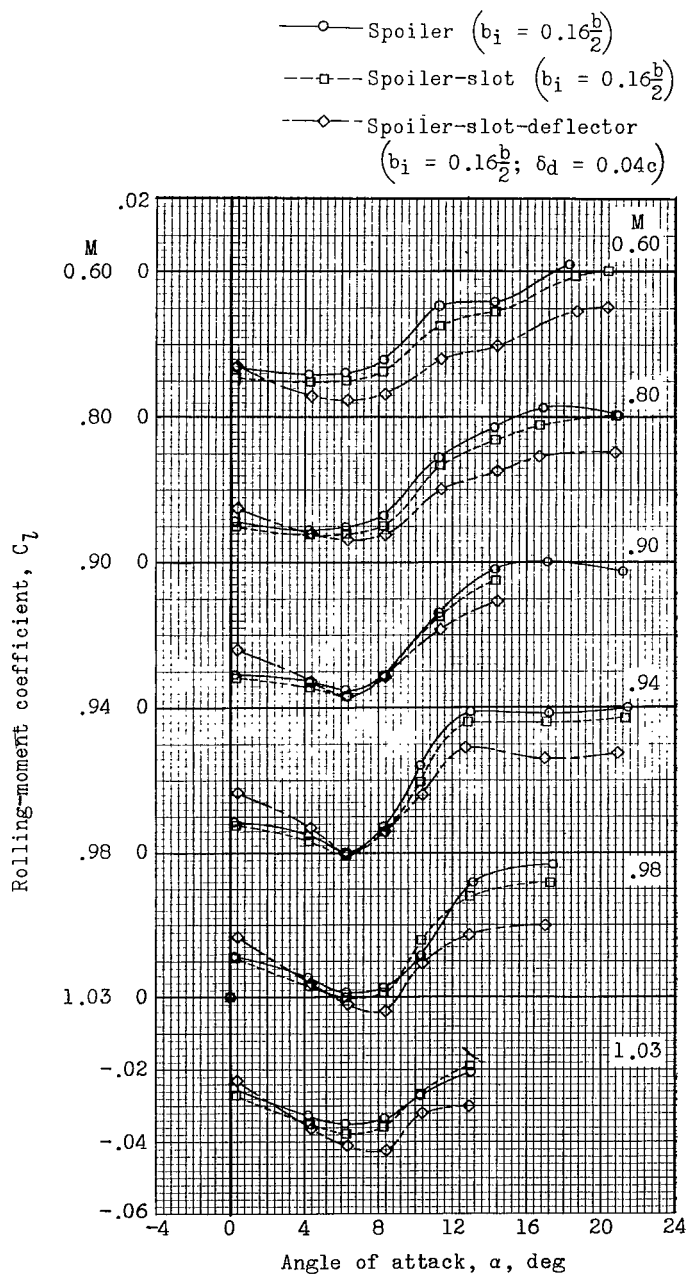
(e) Incremental drag coefficient.

Figure 5.- Continued.



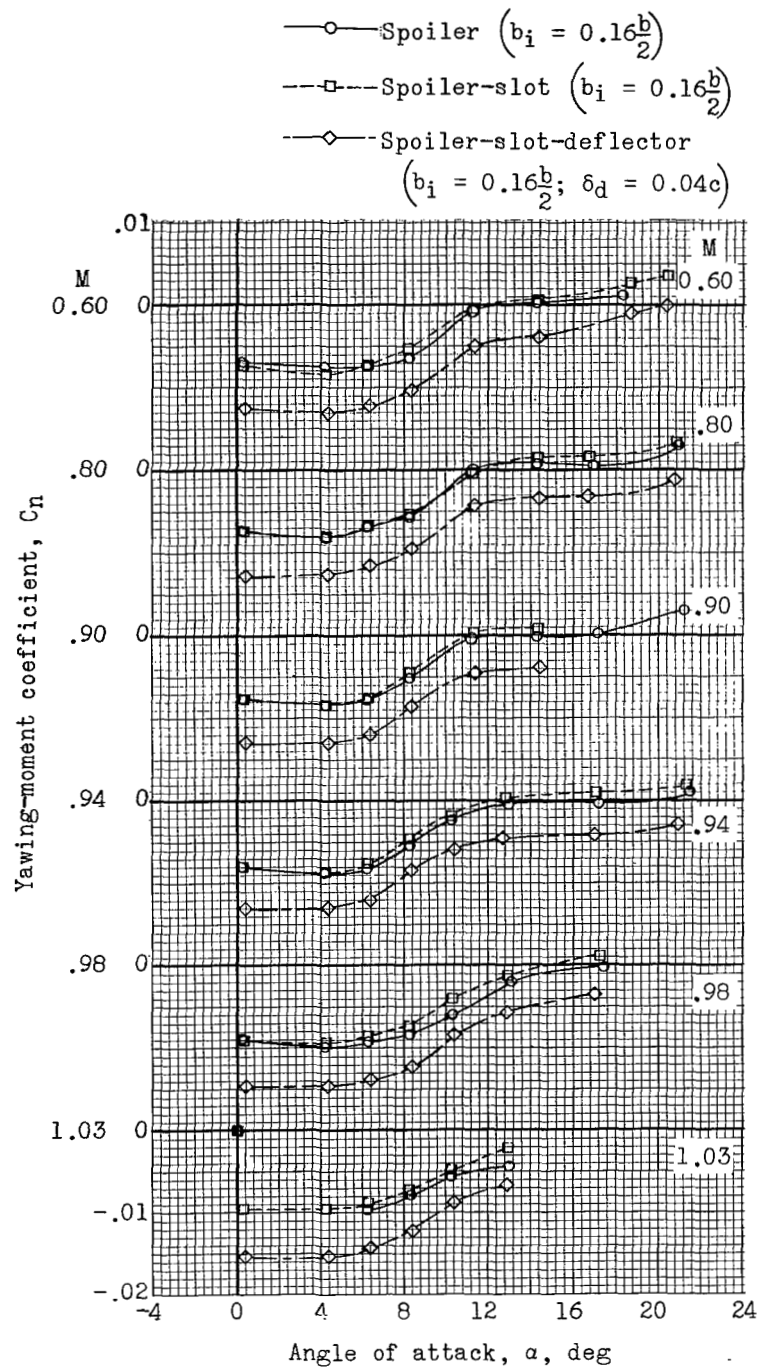
(f) Incremental pitching-moment coefficient.

Figure 5.- Concluded.



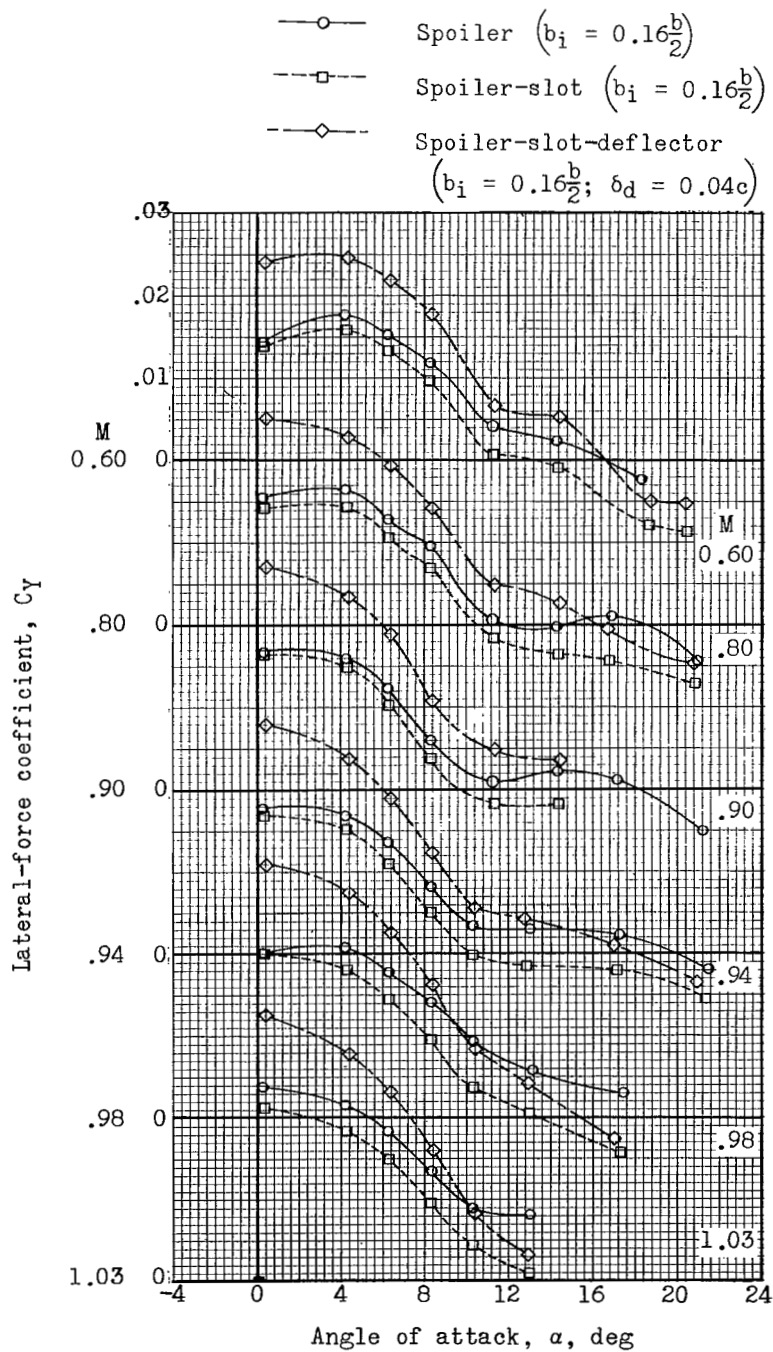
(a) Rolling-moment coefficient.

Figure 6.- Aerodynamic characteristics of spoiler configurations showing effects of adding a wing slot and a wing slot-deflector behind a flap-type spoiler.



(b) Yawing-moment coefficient.

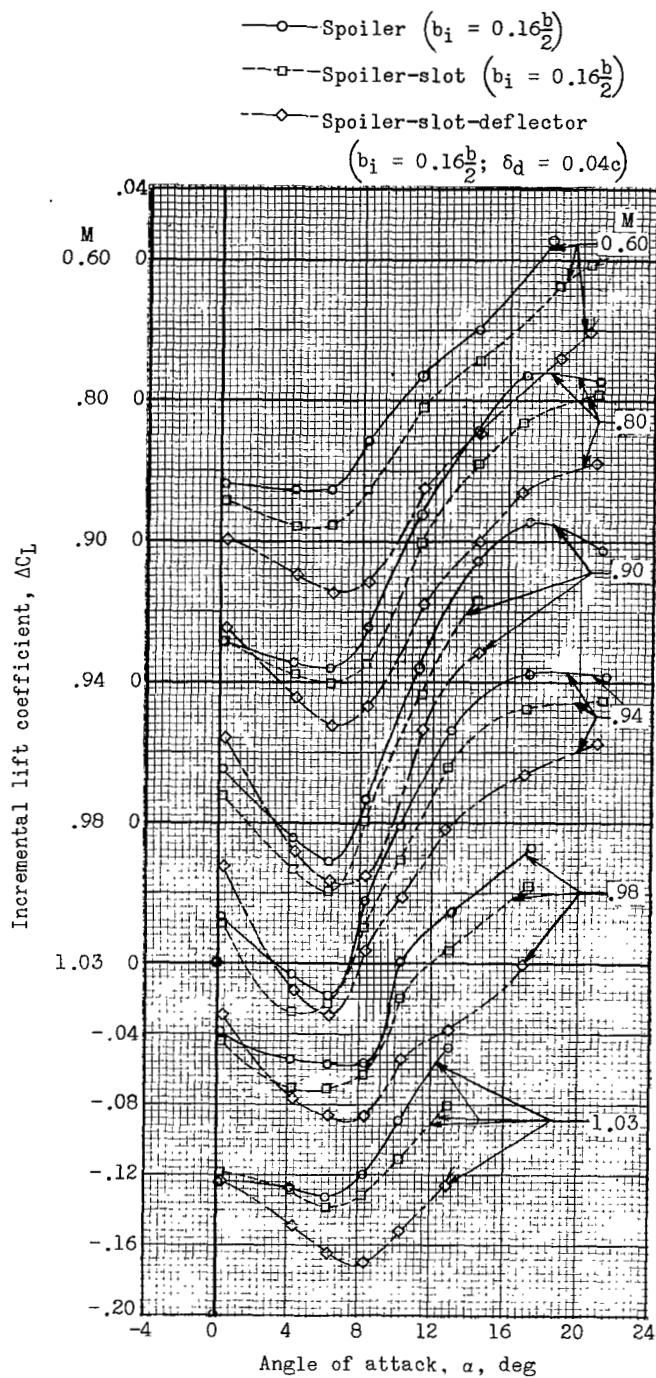
Figure 6.- Continued.



(c) Lateral-force coefficient.

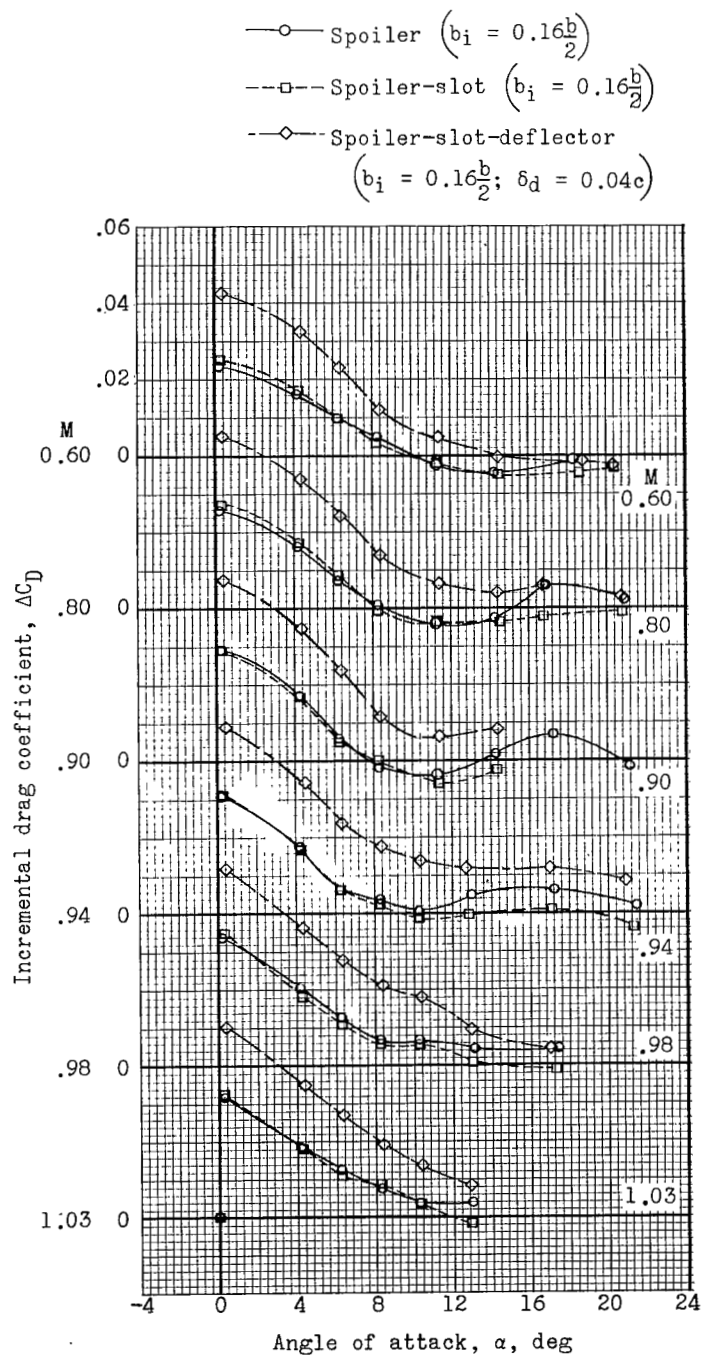
Figure 6.- Continued.





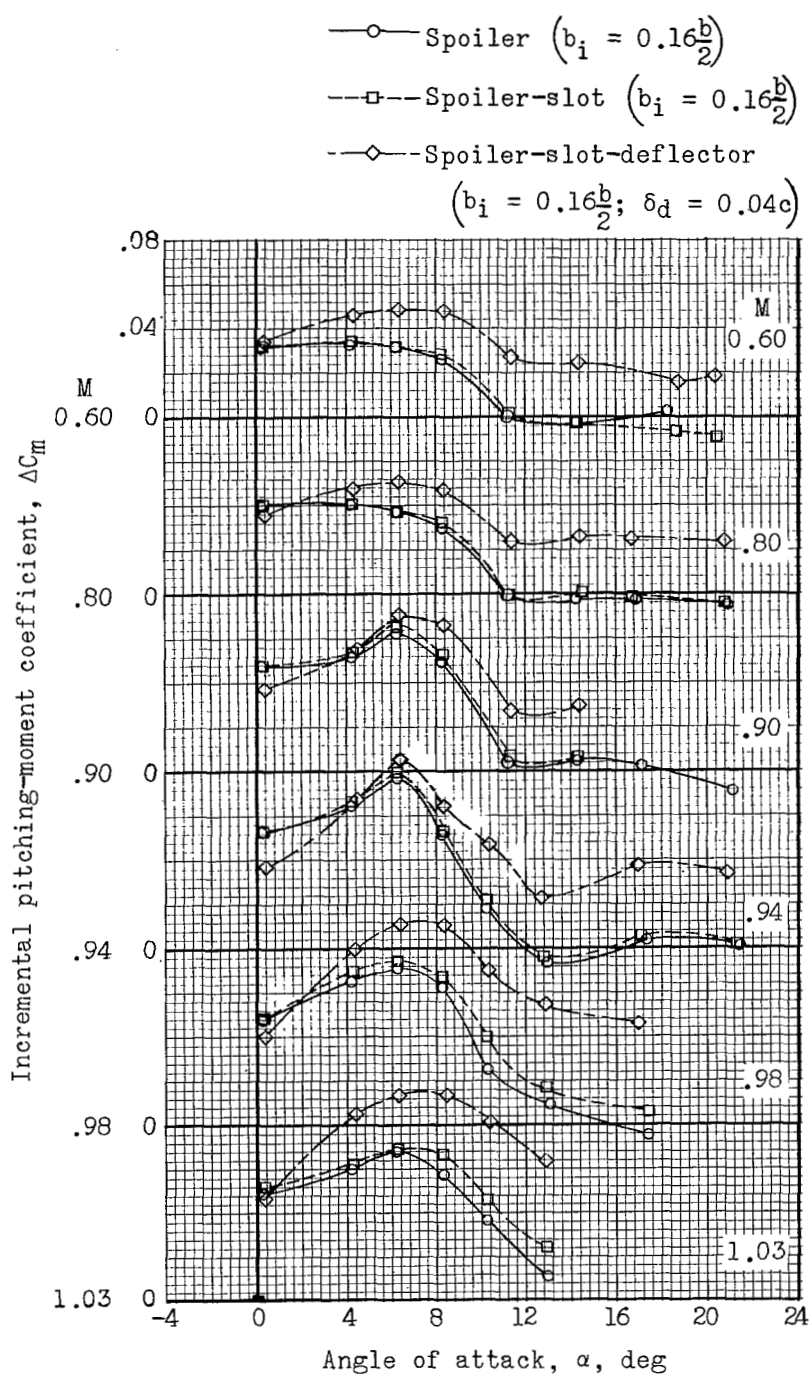
(d) Incremental lift coefficient.

Figure 6.- Continued.



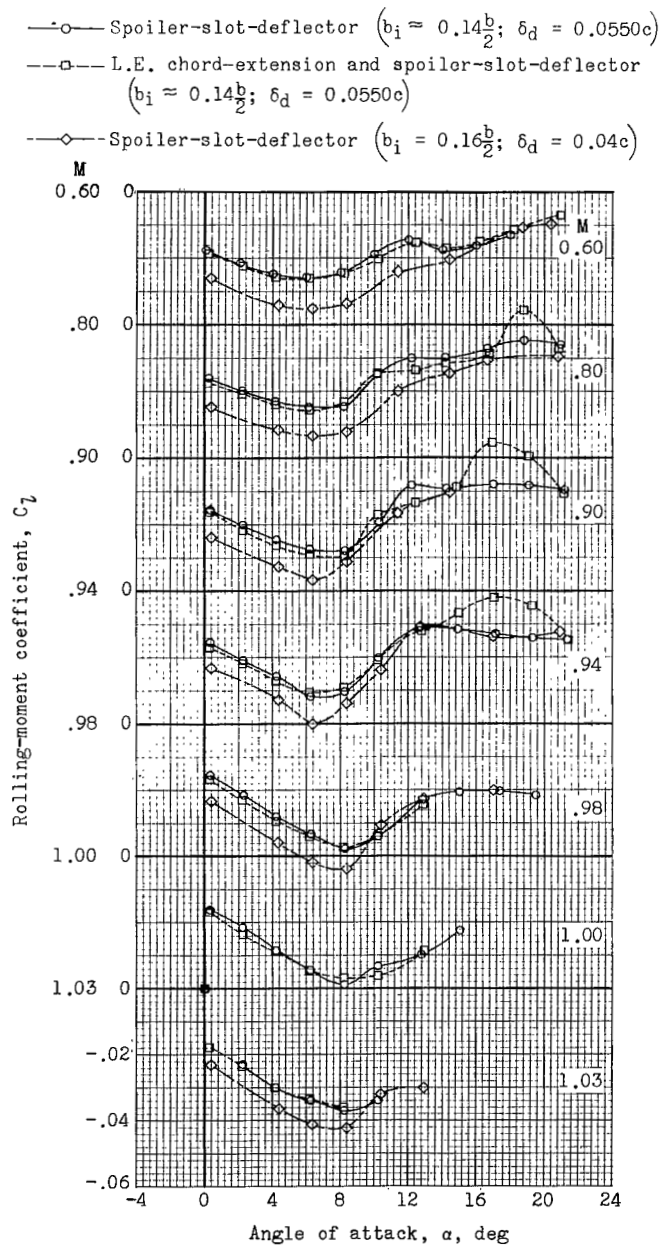
(e) Incremental drag coefficient.

Figure 6.- Continued.



(f) Incremental pitching-moment coefficient.

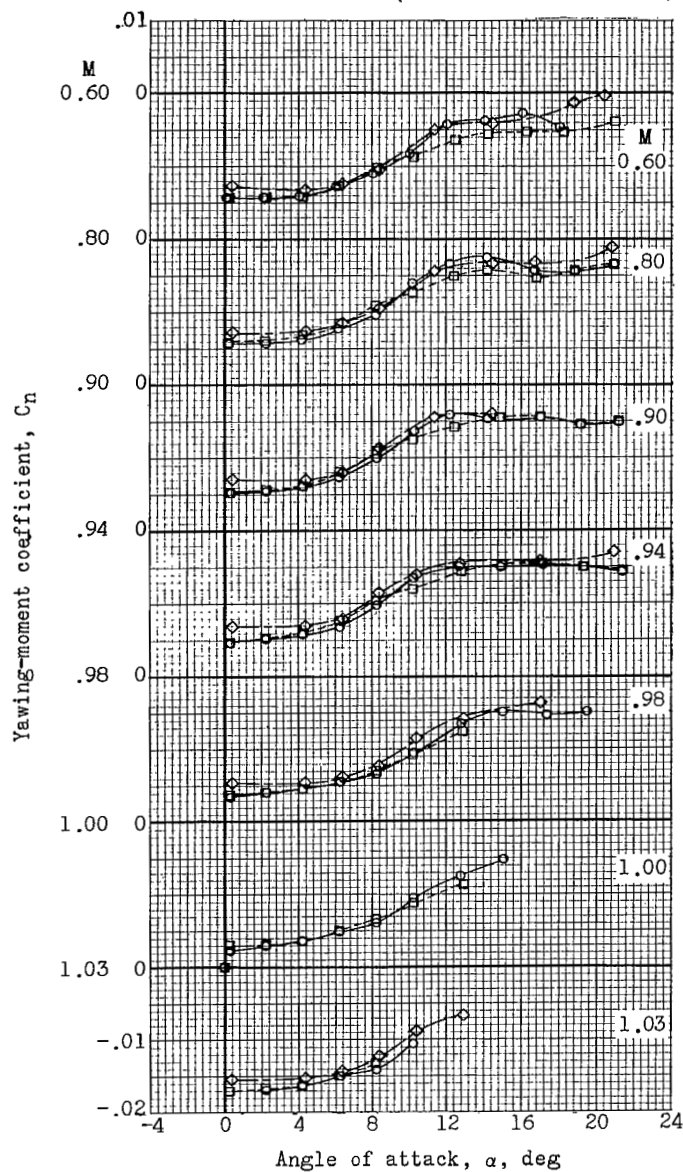
Figure 6.- Concluded.



(a) Rolling-moment coefficient.

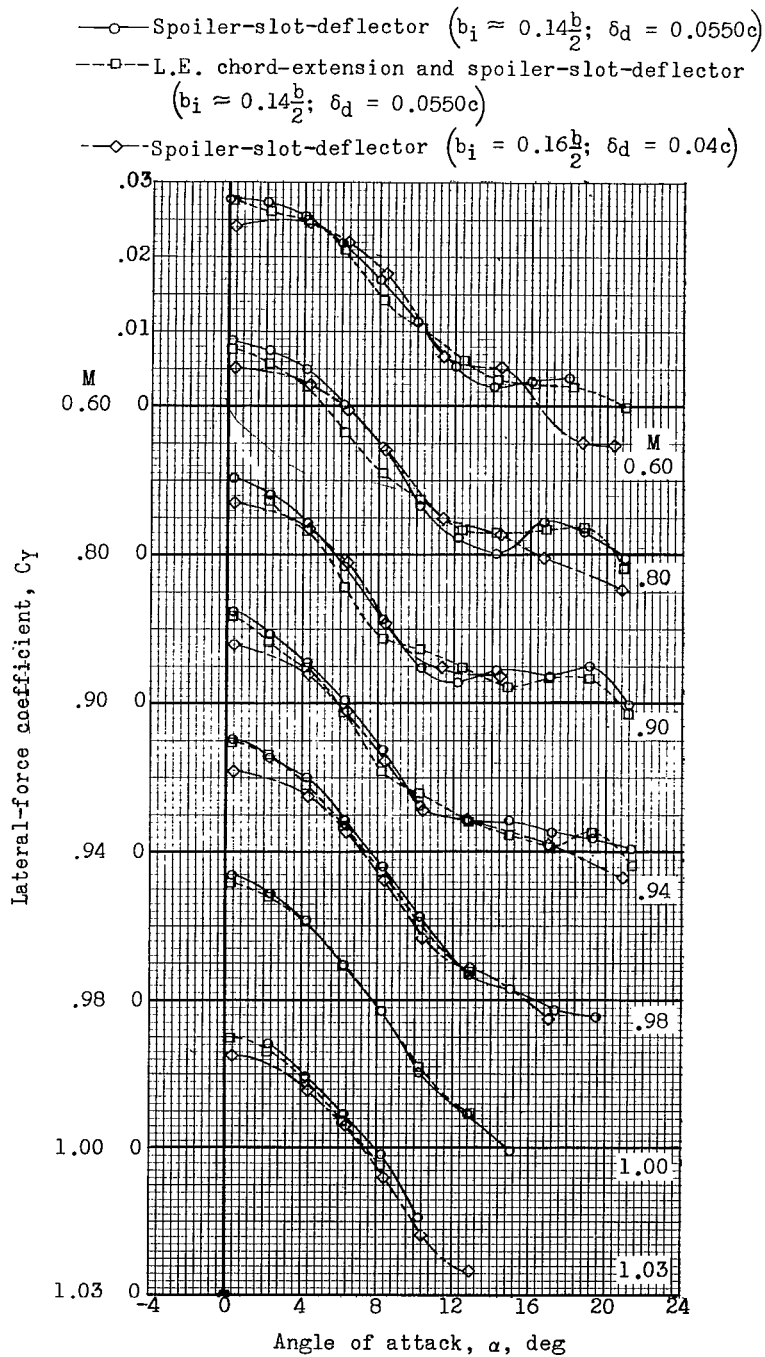
Figure 7.- Aerodynamic characteristics of spoiler-slot-deflector configurations showing effects of adding leading-edge chord-extensions to a spoiler-slot-deflector configuration and of changing the spoiler-slot-deflector configuration.

- Spoiler-slot-deflector ( $b_i \approx 0.14\frac{b}{2}$ ;  $\delta_d = 0.0550c$ )
- L.E. chord-extension and spoiler-slot-deflector ( $b_i \approx 0.14\frac{b}{2}$ ;  $\delta_d = 0.0550c$ )
- ◇— Spoiler-slot-deflector ( $b_i = 0.16\frac{b}{2}$ ;  $\delta_d = 0.04c$ )



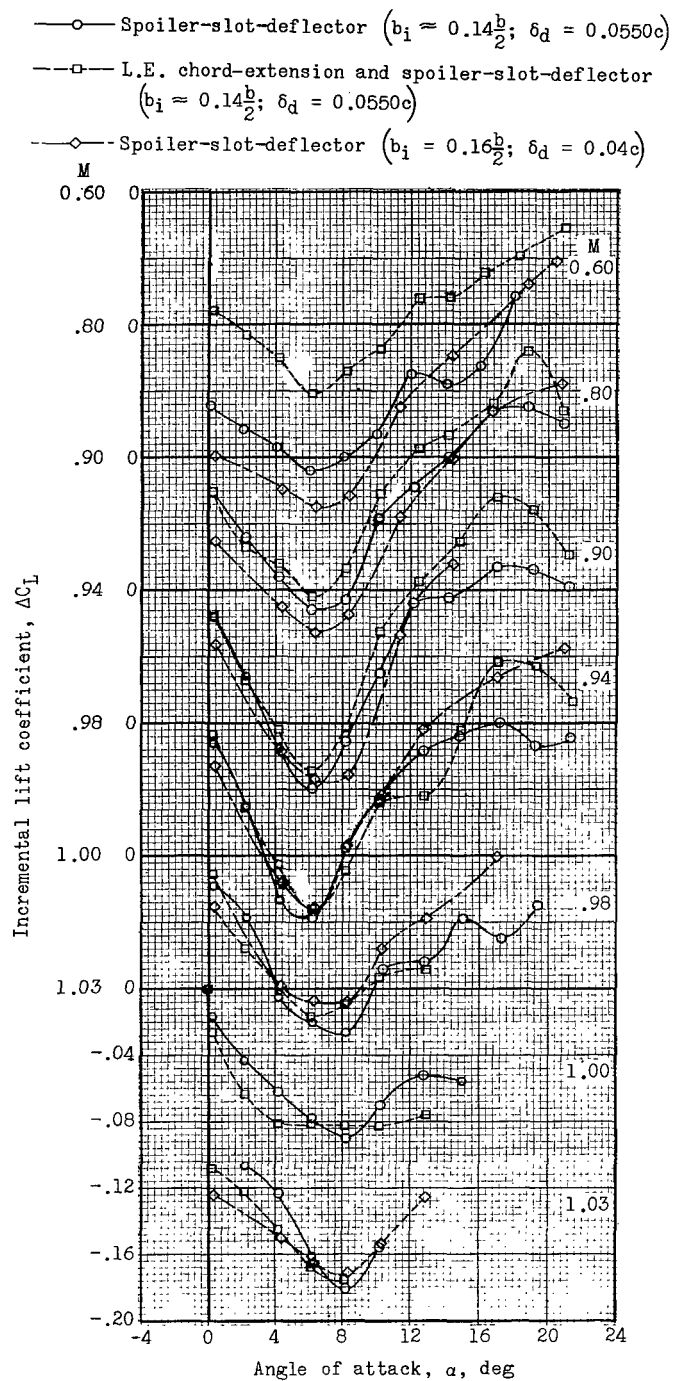
(b) Yawing-moment coefficient.

Figure 7.- Continued.



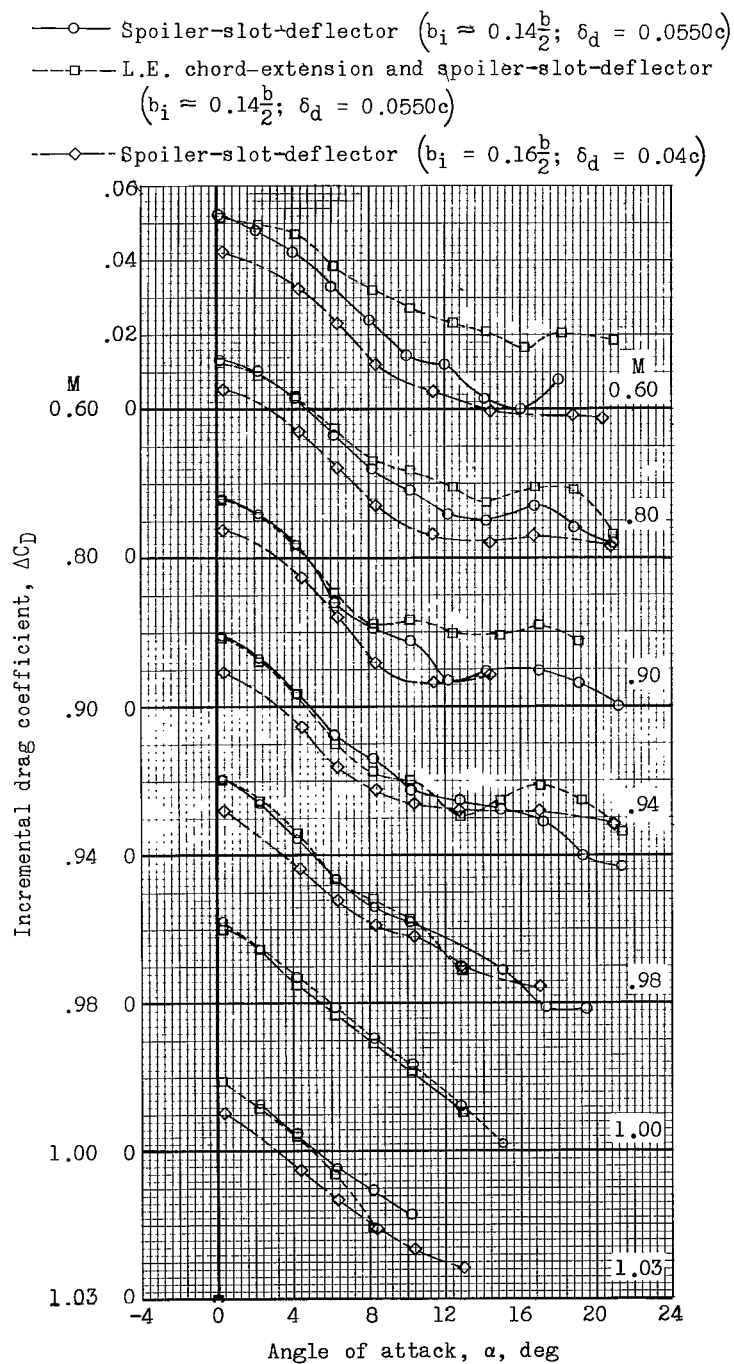
(c) Lateral-force coefficient.

Figure 7.- Continued.



(d) Incremental lift coefficient.

Figure 7.- Continued.

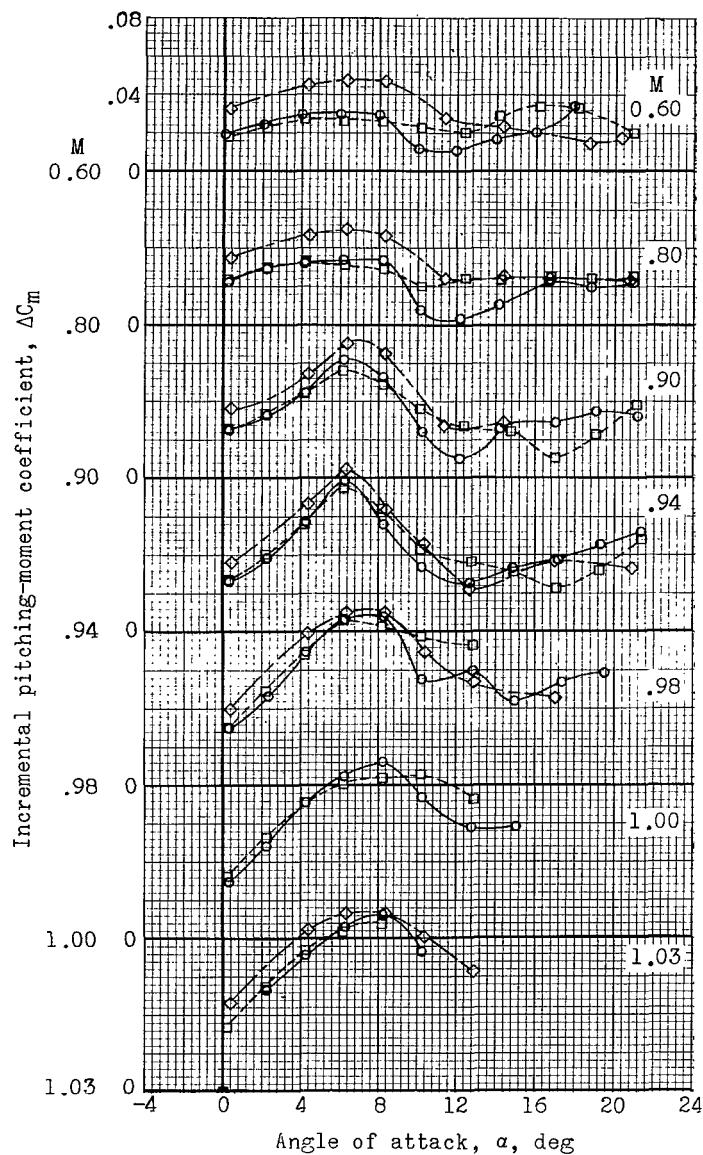


(e) Incremental drag coefficient.

Figure 7.- Continued.

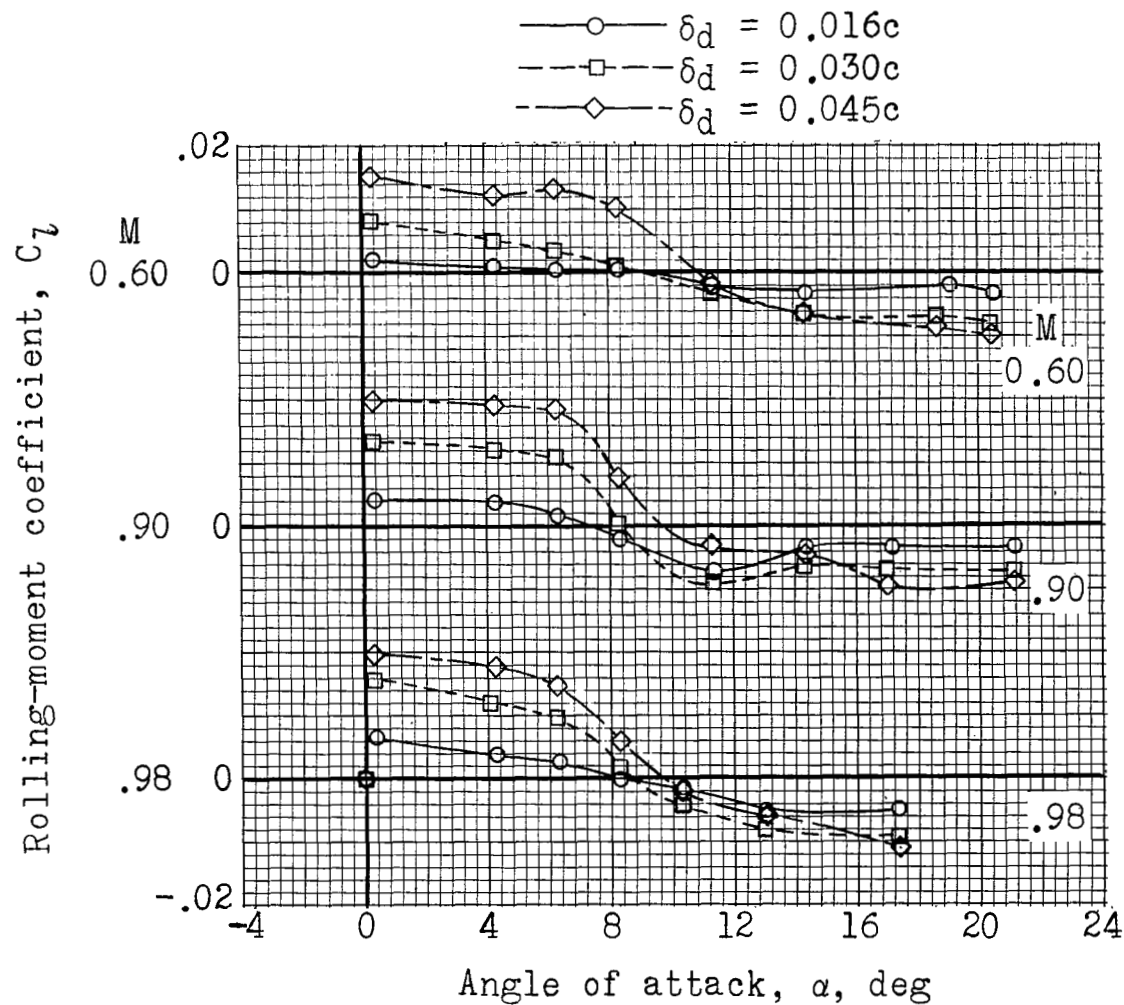


- Spoiler-slot-deflector ( $b_i \approx 0.14\frac{b}{2}$ ;  $\delta_d = 0.0550c$ )  
 ---□--- L.E. chord-extension and spoiler-slot-deflector  
 ( $b_i \approx 0.14\frac{b}{2}$ ;  $\delta_d = 0.0550c$ )  
 ---◇--- Spoiler-slot-deflector ( $b_i = 0.16\frac{b}{2}$ ;  $\delta_d = 0.04c$ )



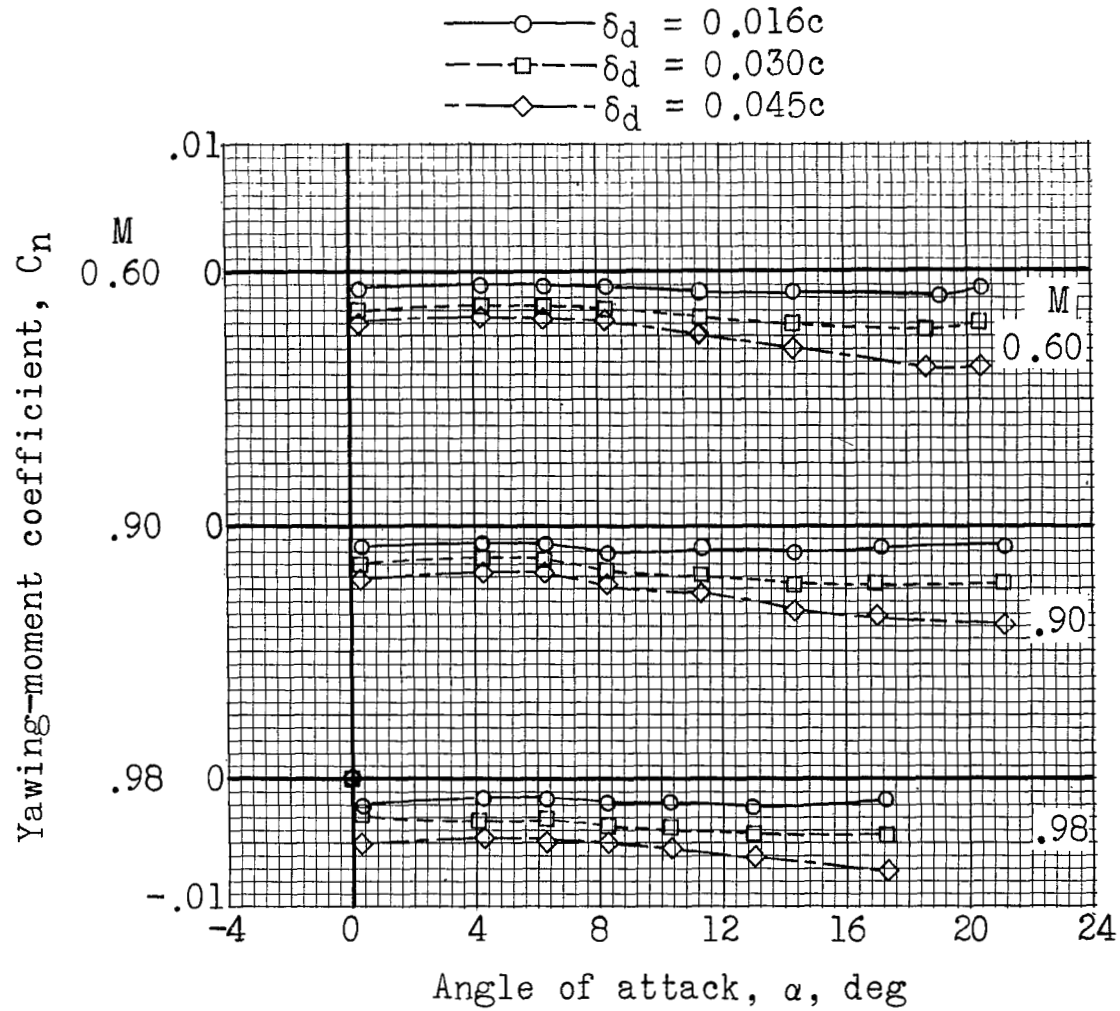
(f) Incremental pitching-moment coefficient.

Figure 7.- Concluded.



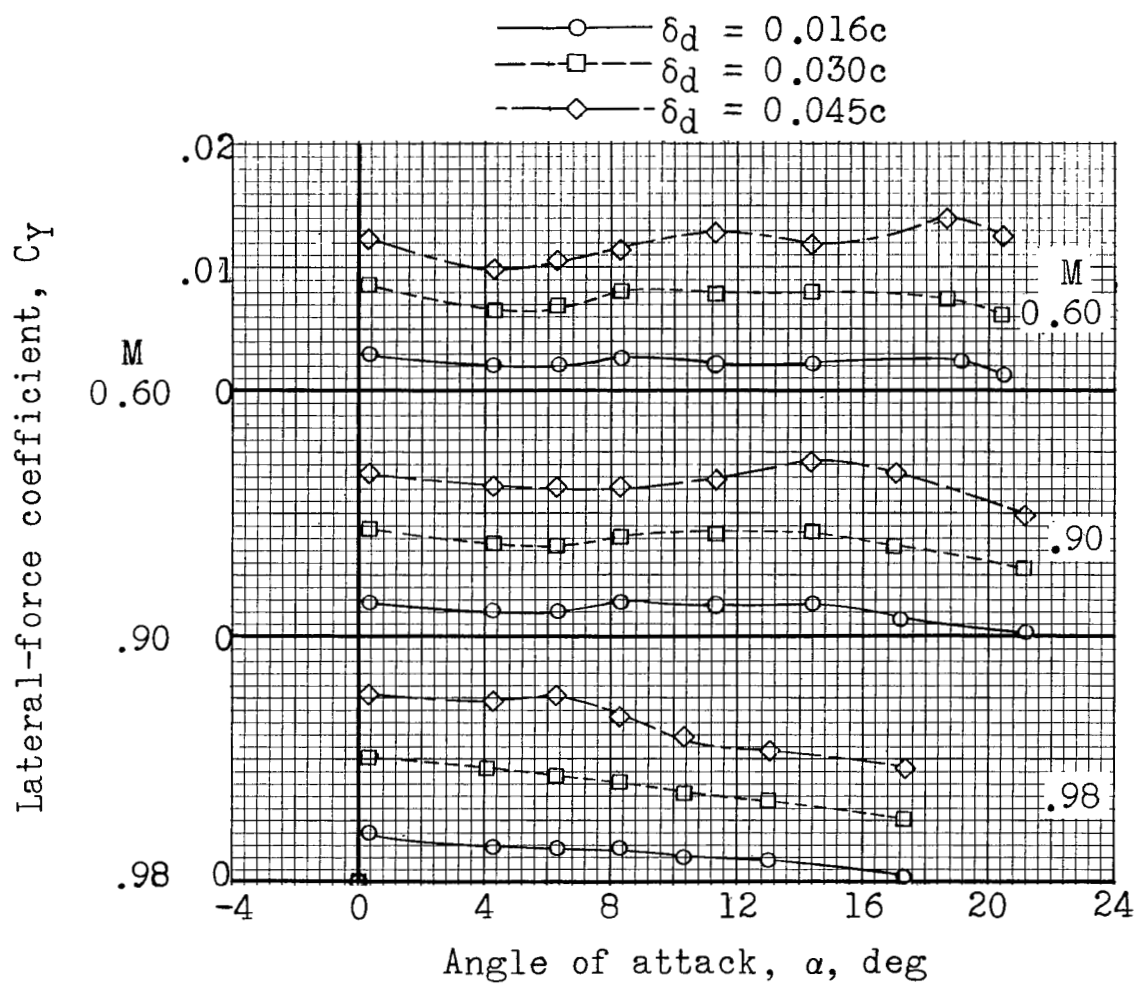
(a) Rolling-moment coefficient.

Figure 8.- Aerodynamic characteristics of deflector configurations showing the effect of deflector projection.



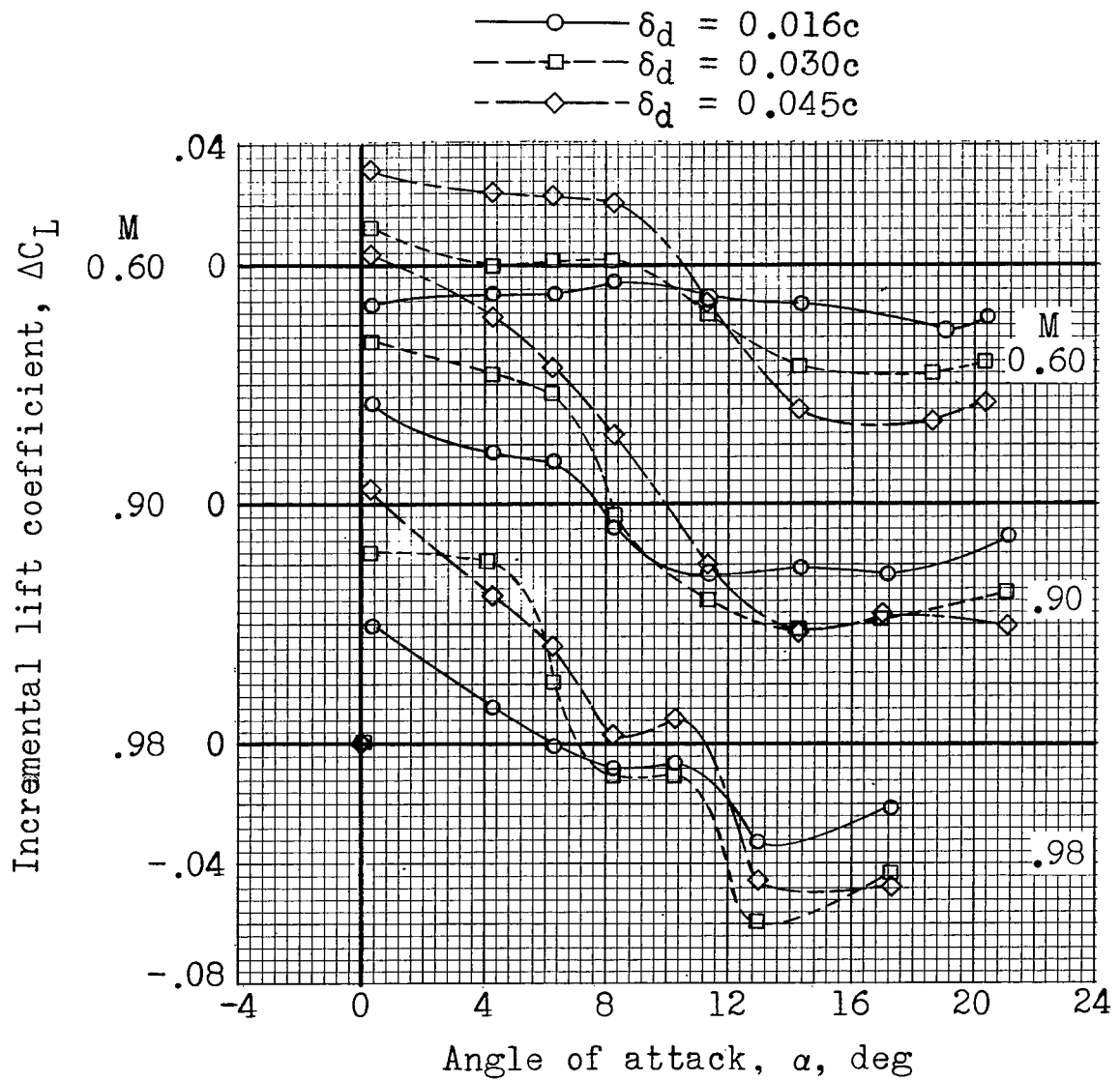
(b) Yawing-moment coefficient.

Figure 8.- Continued.



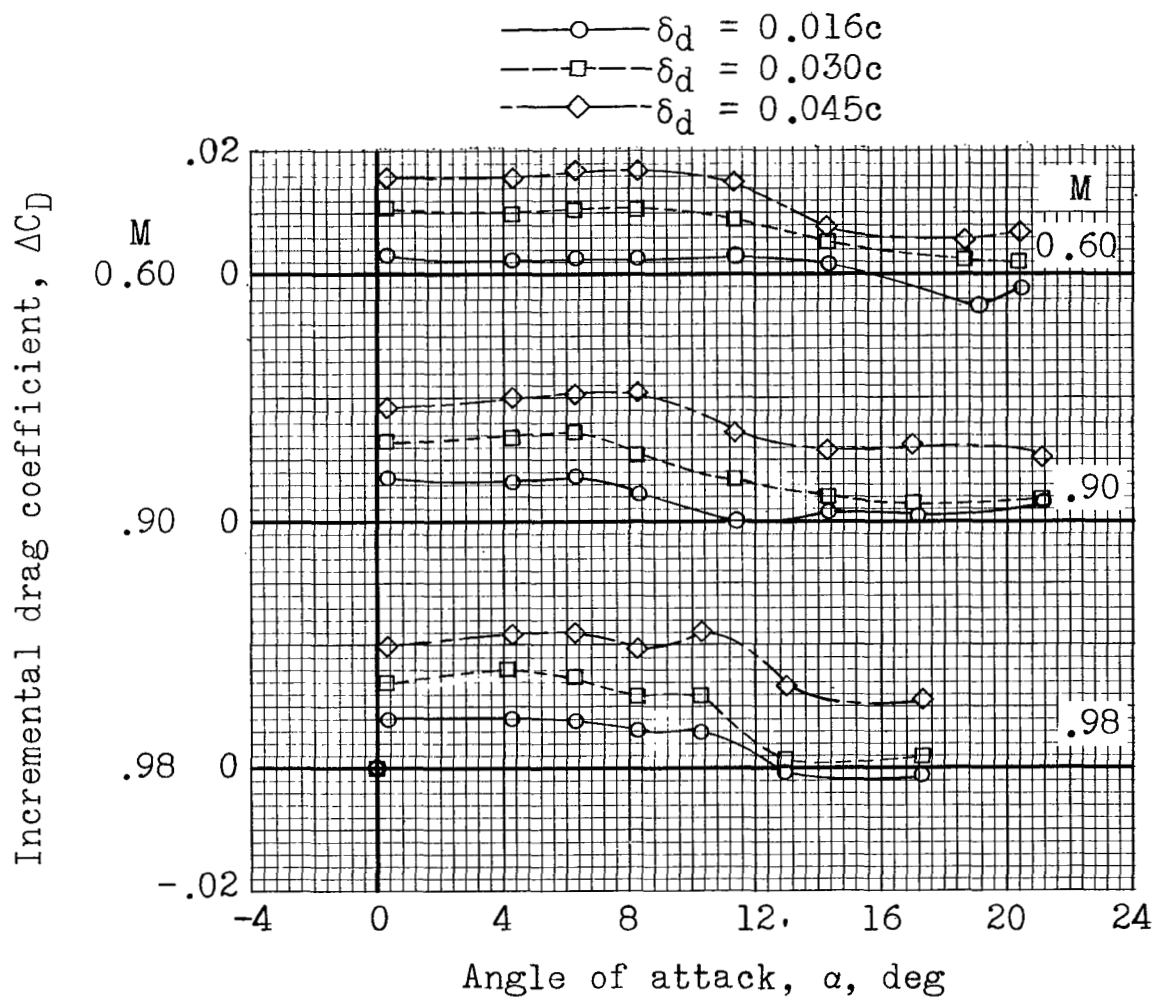
(c) Lateral-force coefficient.

Figure 8.- Continued.



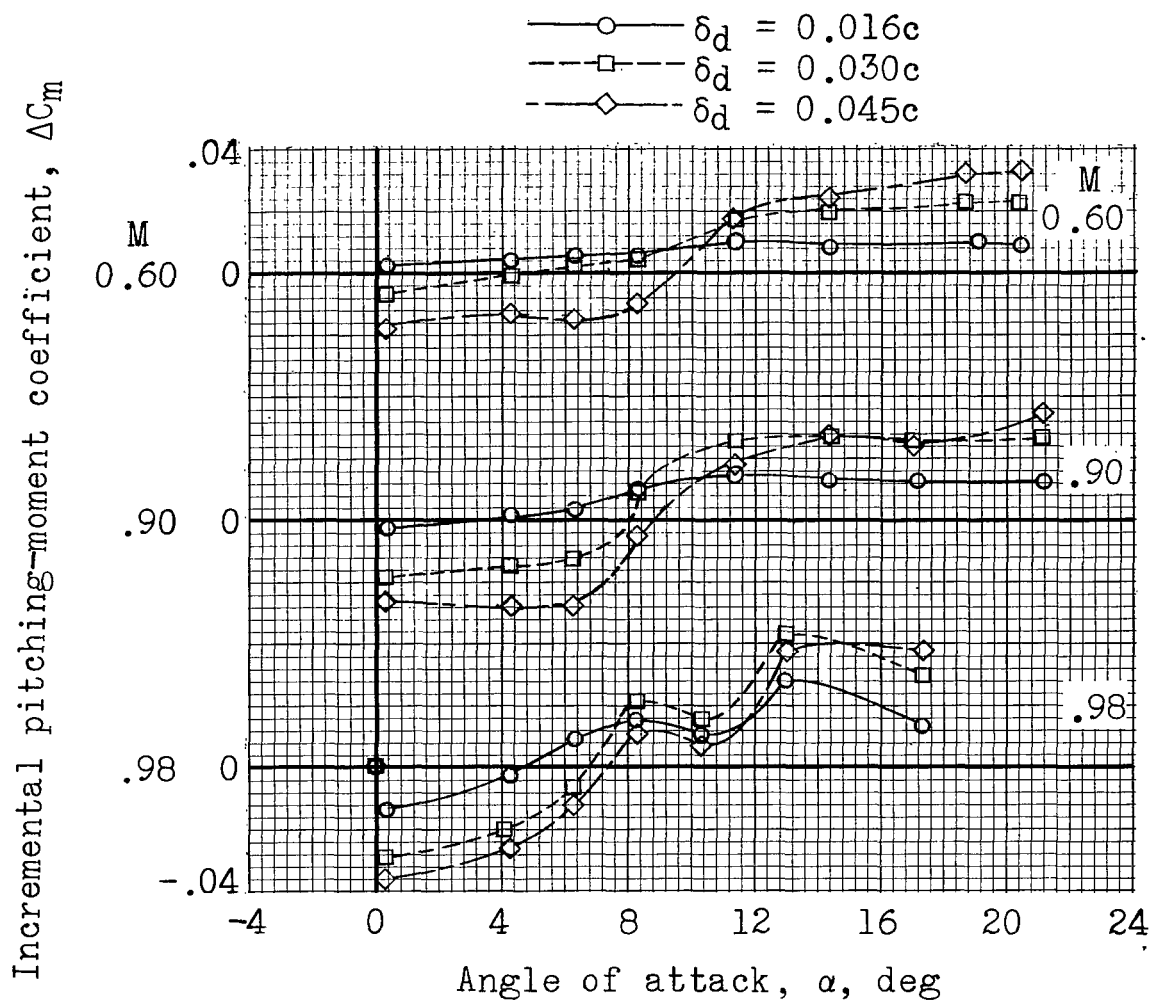
(d) Incremental lift coefficient.

Figure 8.- Continued.



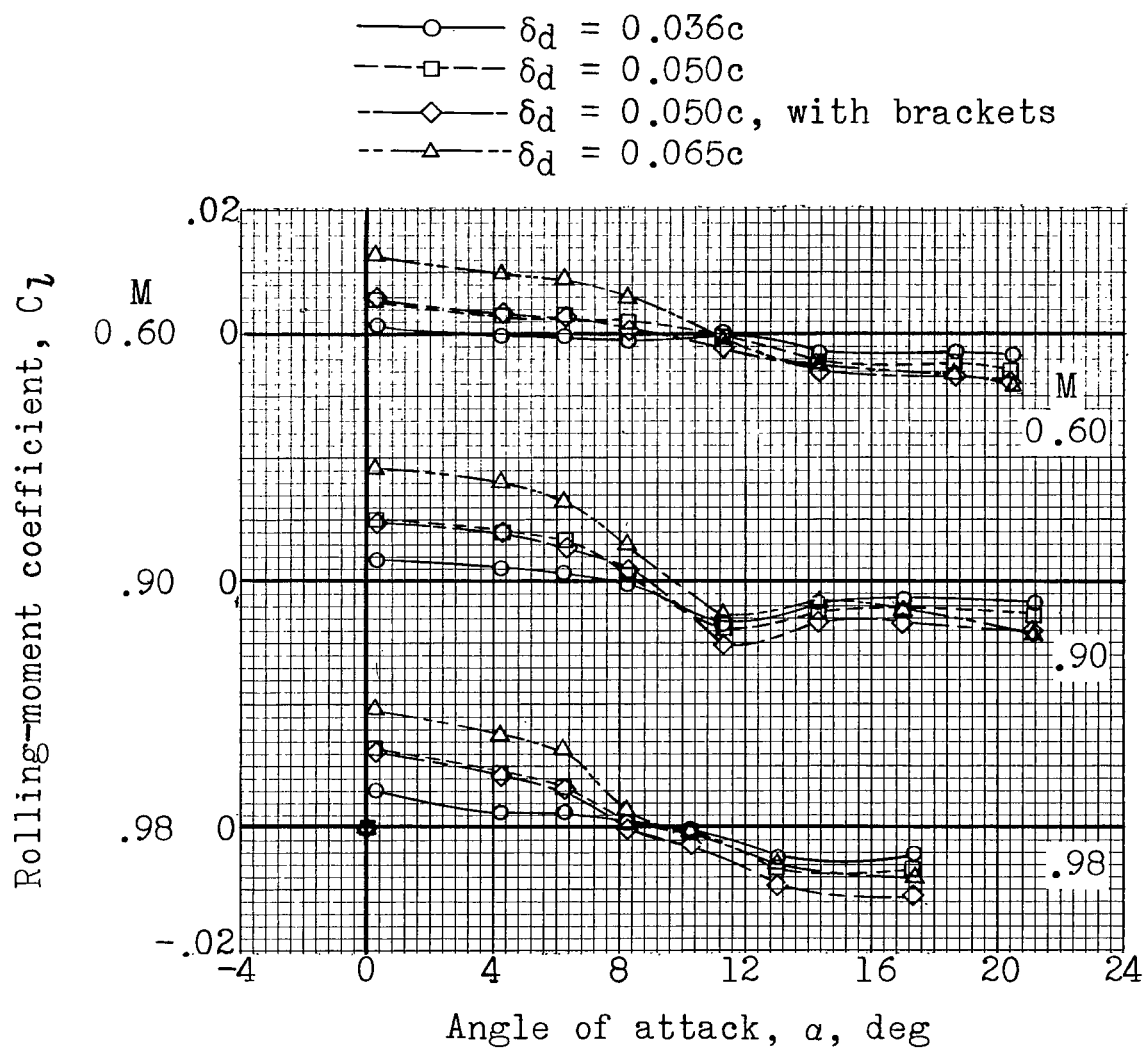
(e) Incremental drag coefficient.

Figure 8.- Continued.



(f) Incremental pitching-moment coefficient.

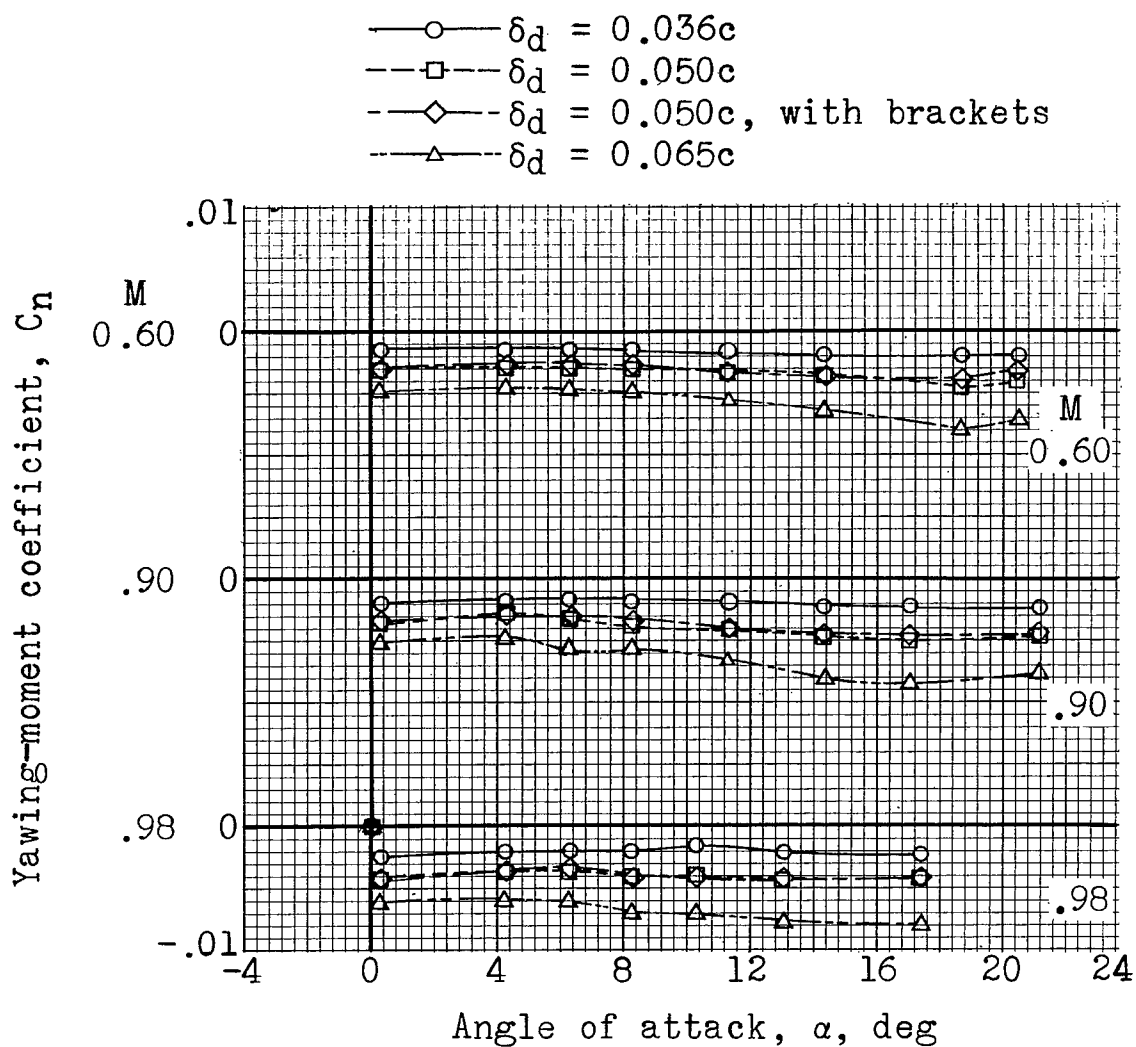
Figure 8.- Concluded.



(a) Rolling-moment coefficient.

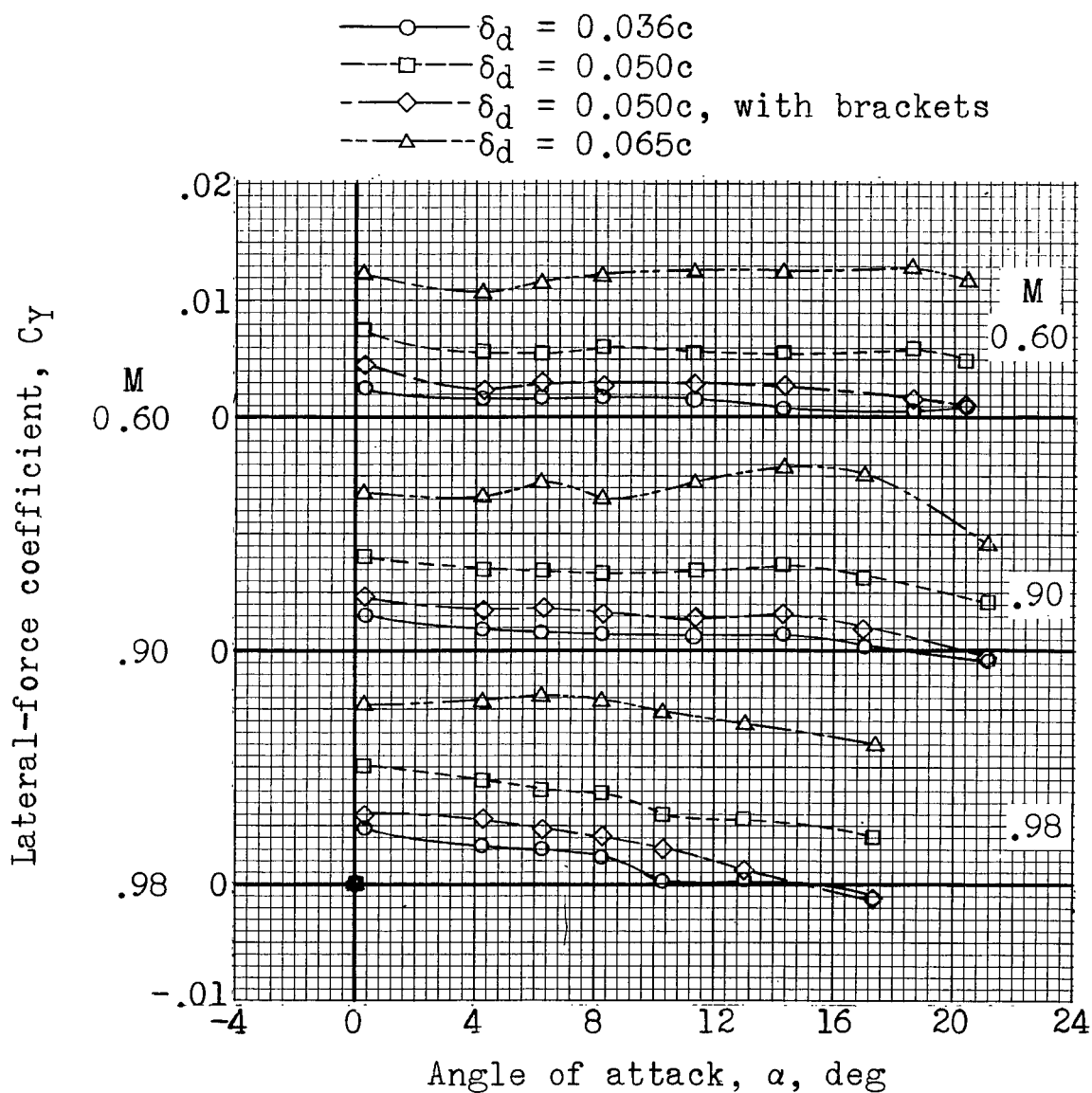
Figure 9.- Aerodynamic characteristics of deflector configurations with a 0.02 gap between wing and deflector showing effects of deflector projection and deflector brackets.





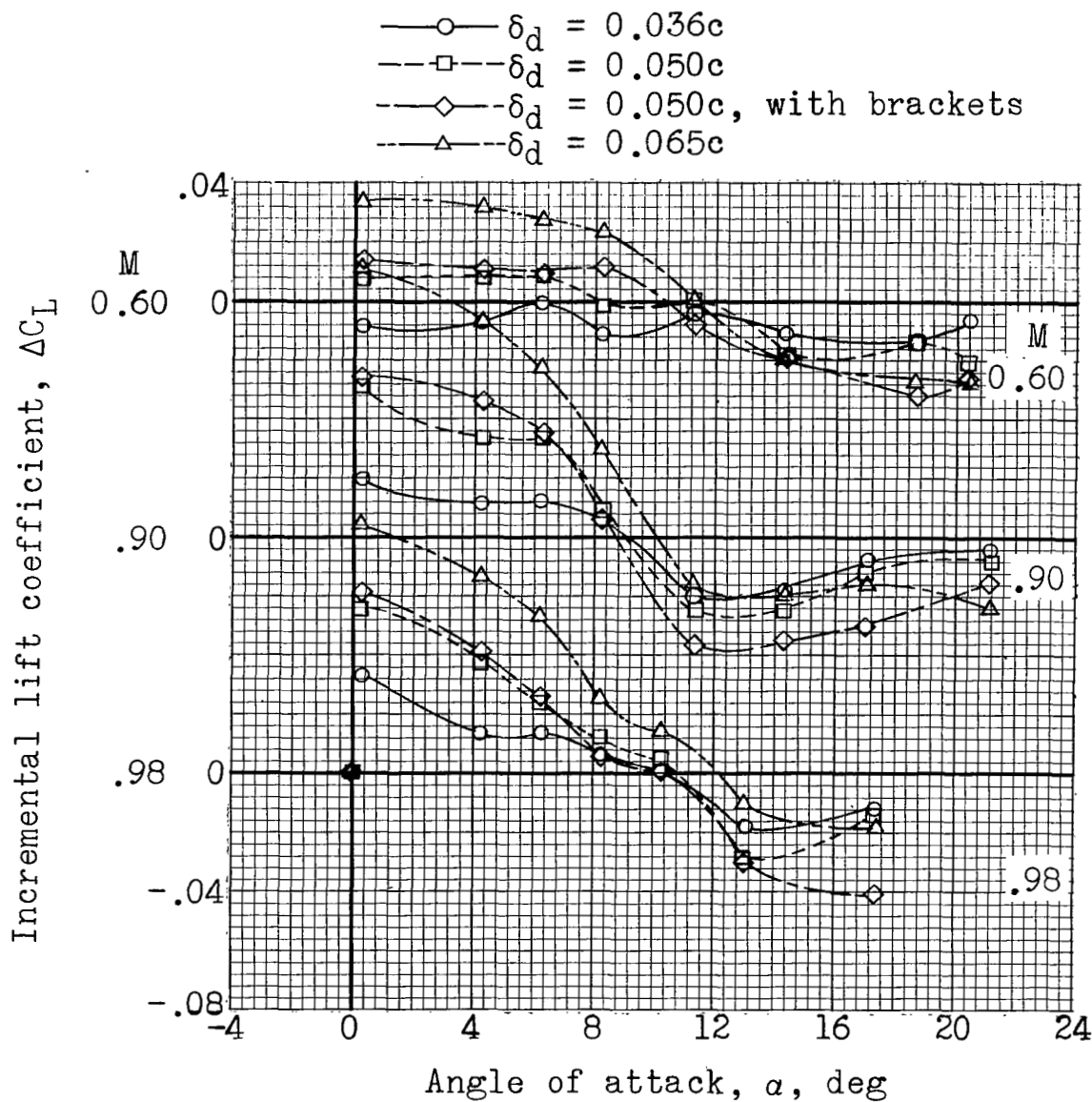
(b) Yawing-moment coefficient.

Figure 9.- Continued.



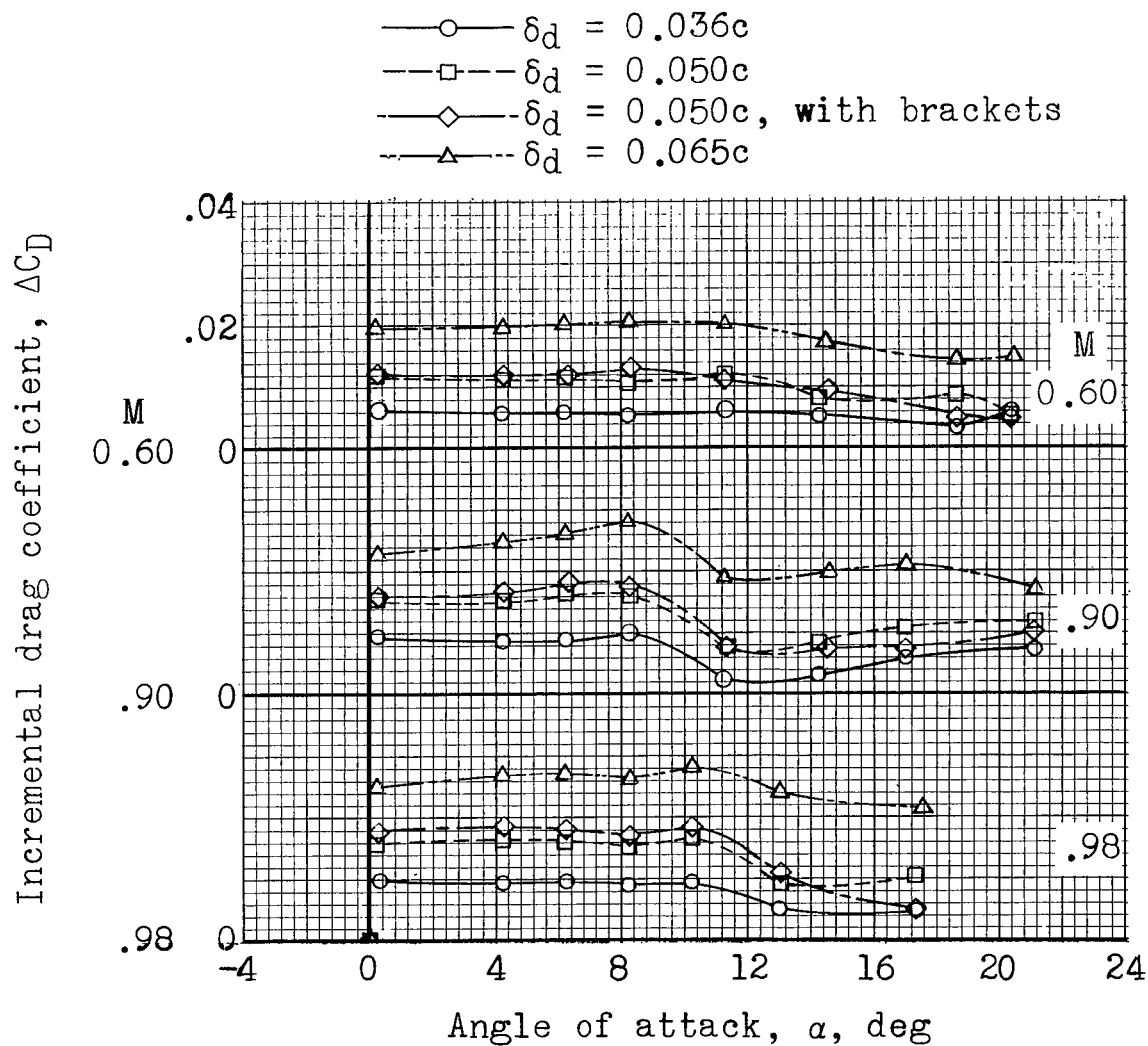
(c) Lateral-force coefficient.

Figure 9.- Continued.



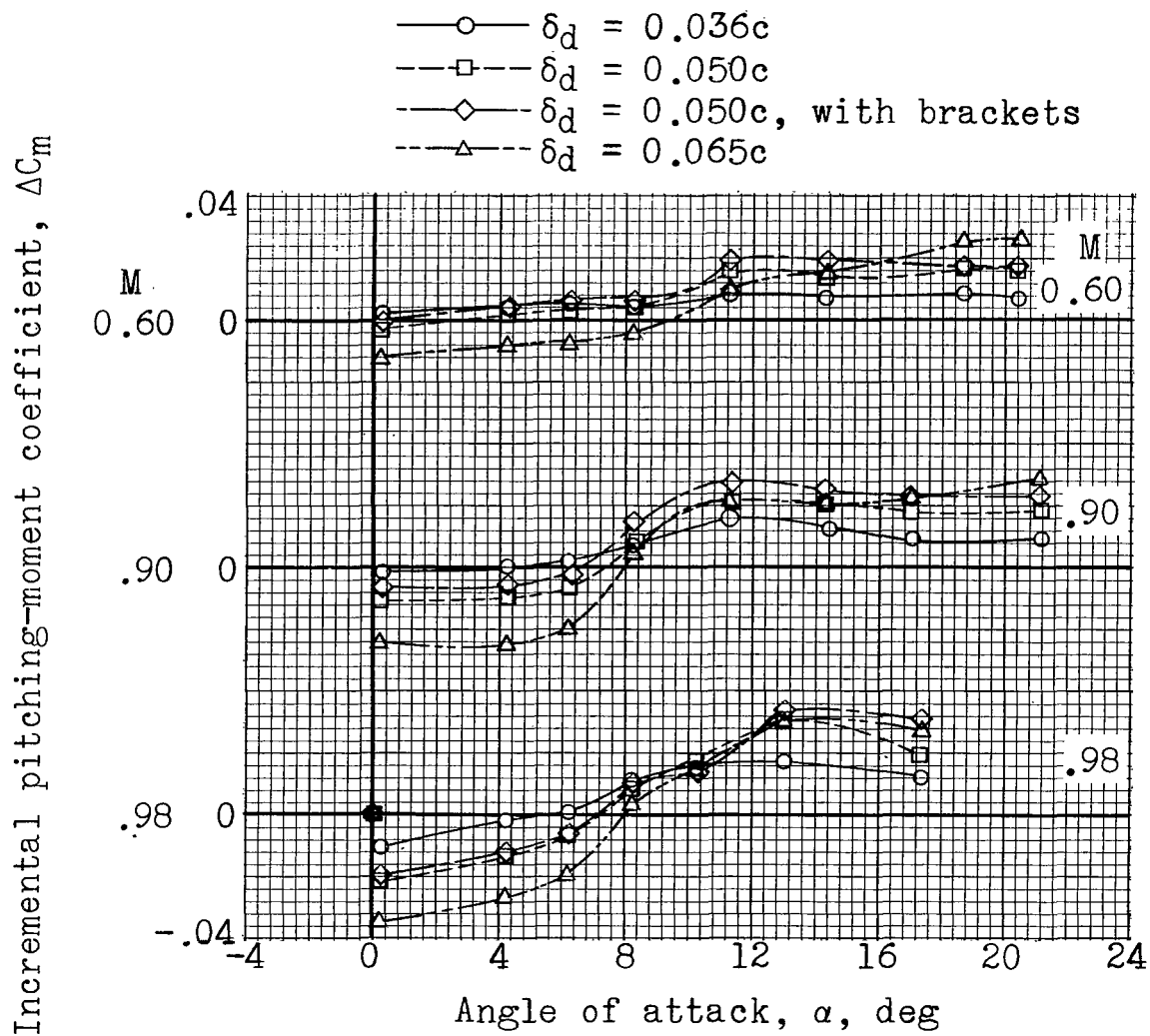
(d) Incremental lift coefficient.

Figure 9.- Continued.



(e) Incremental drag coefficient.

Figure 9.- Continued.



(f) Incremental pitching-moment coefficient.

Figure 9.- Concluded.

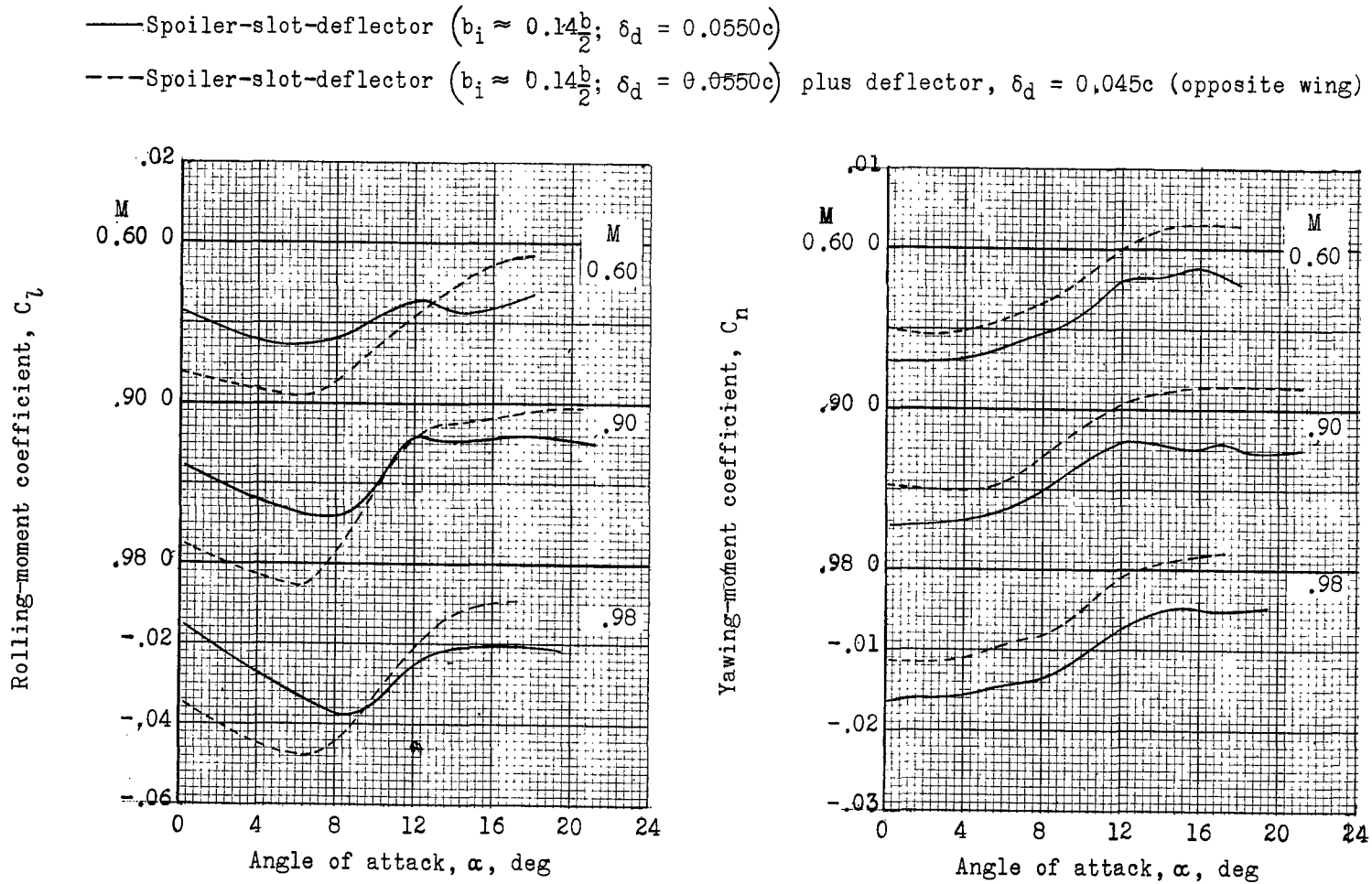
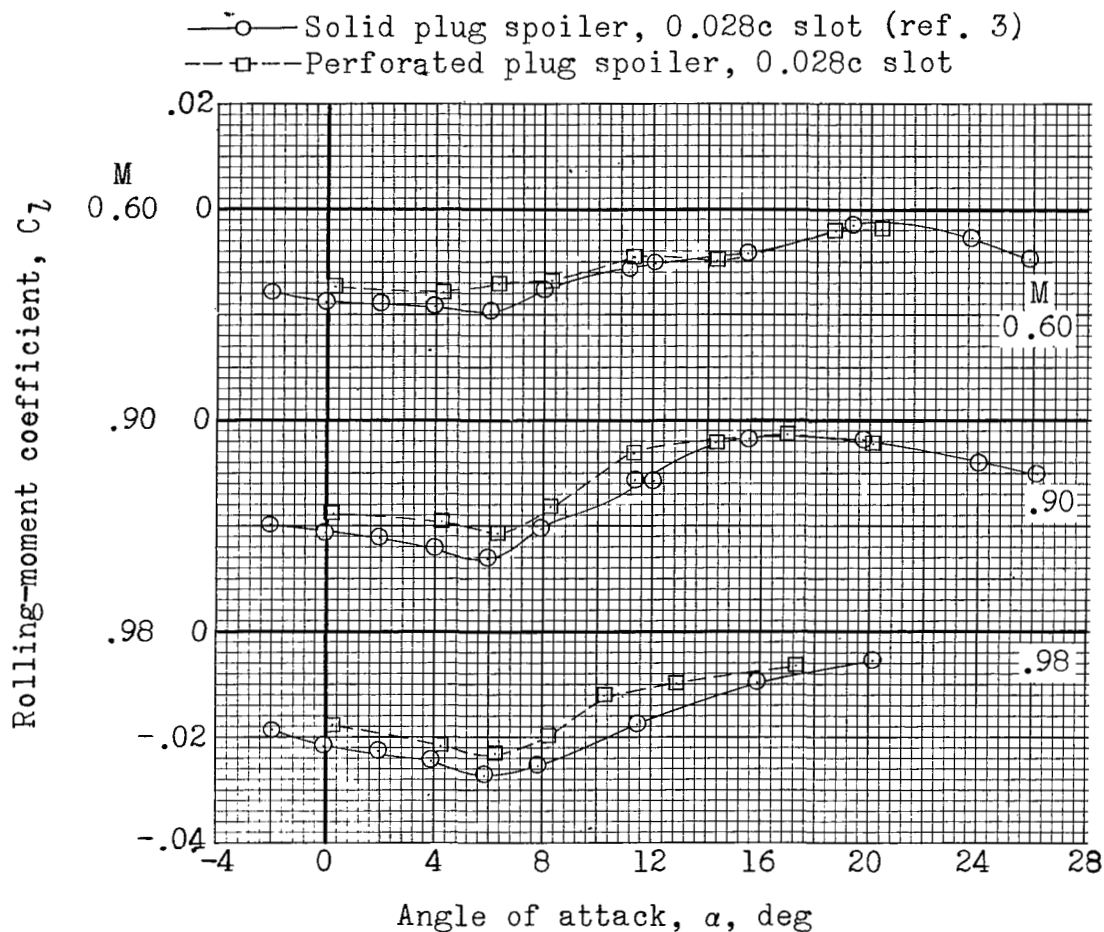
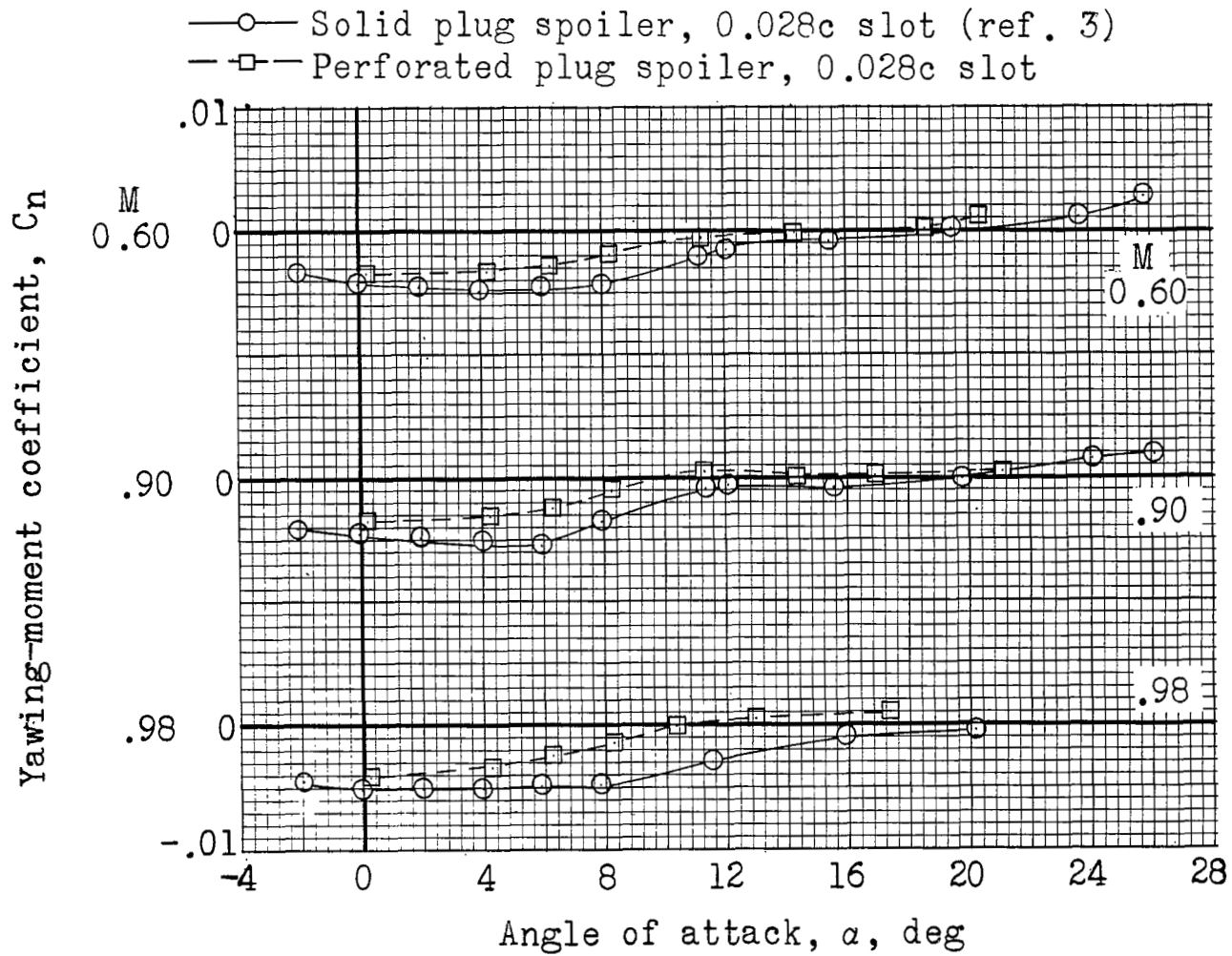


Figure 10.- Effect on rolling-moment and yawing-moment coefficients of adding a deflector to opposite wing panel of a spoiler-slot-deflector configuration.



(a) Rolling-moment coefficient.

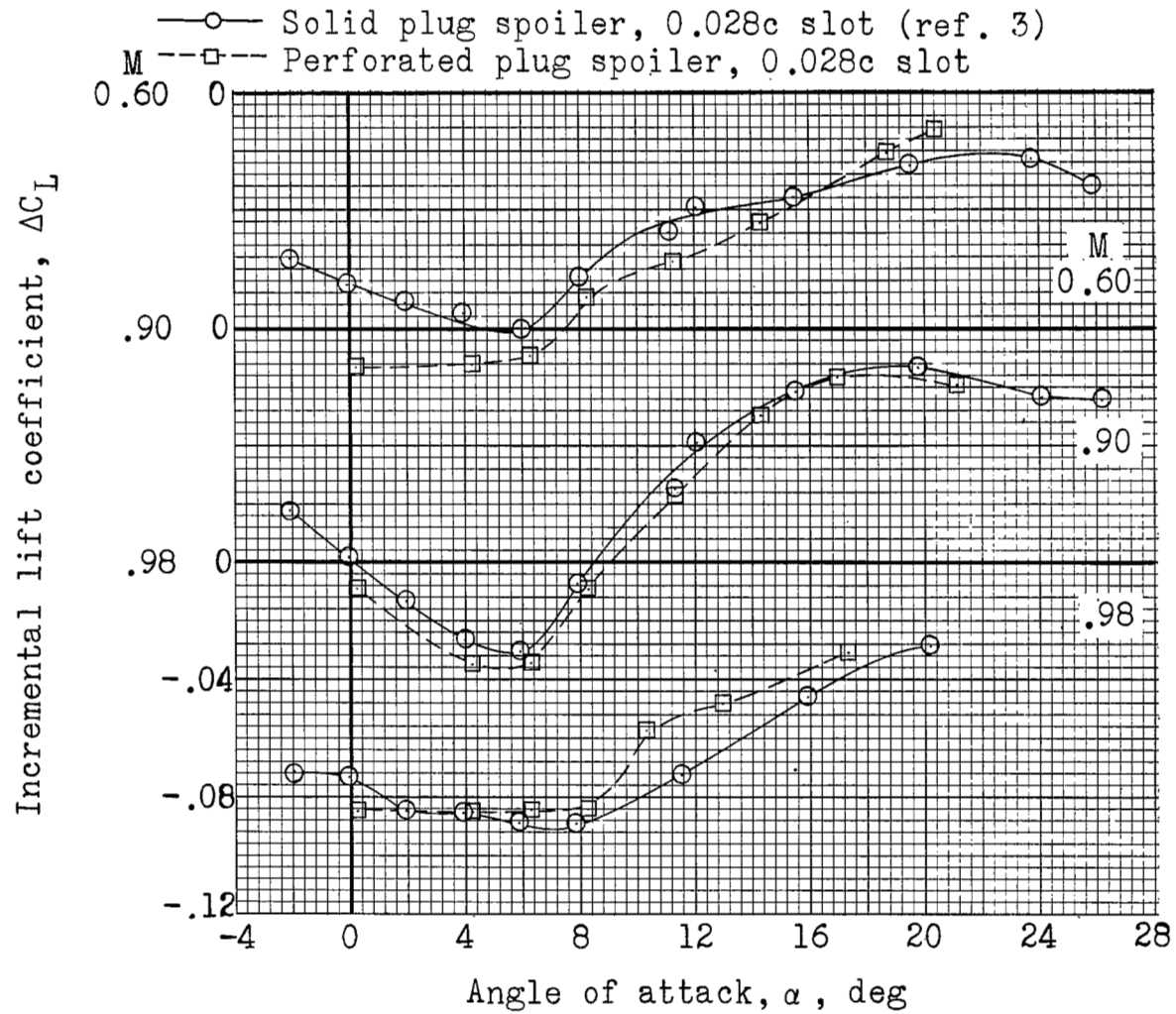
Figure 11.- Aerodynamic characteristics of plug spoiler configurations showing the effect of perforations in the spoiler.



(b) Yawing-moment coefficient.

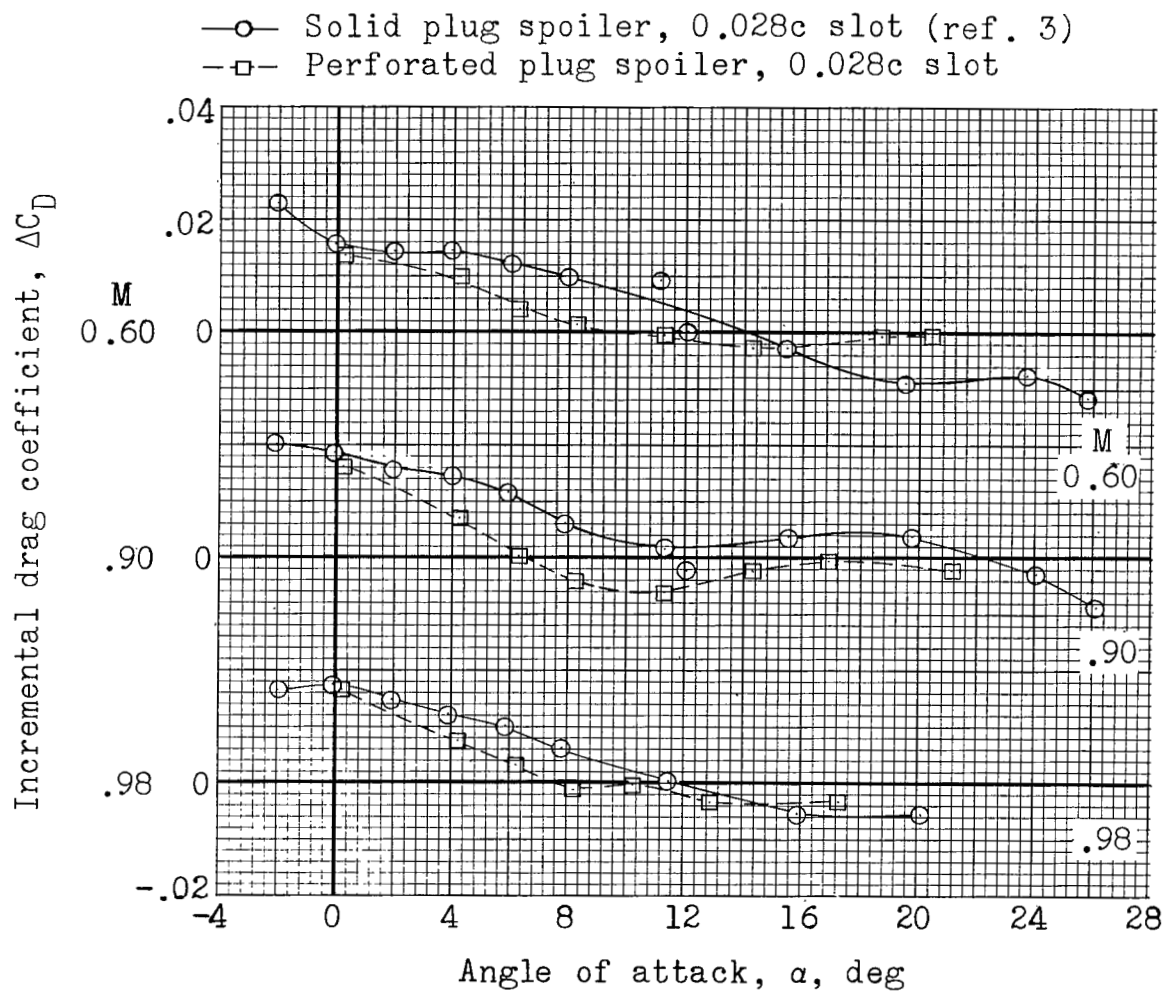
Figure 11.- Continued.





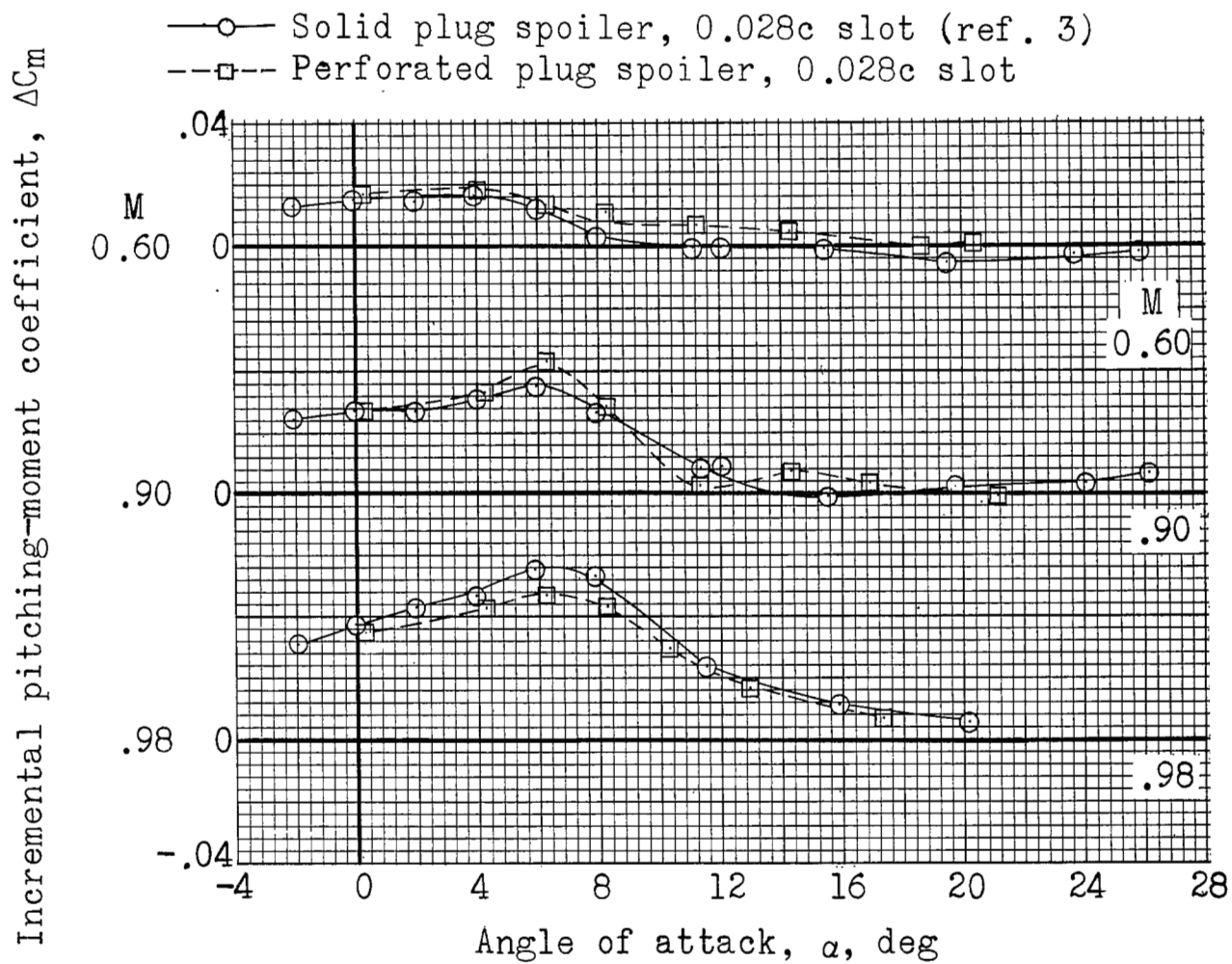
(c) Incremental lift coefficient.

Figure 11.- Continued.



(d) Incremental drag coefficient.

Figure 11.- Continued.



(e) Incremental pitching-moment coefficient.

Figure 11.- Concluded.

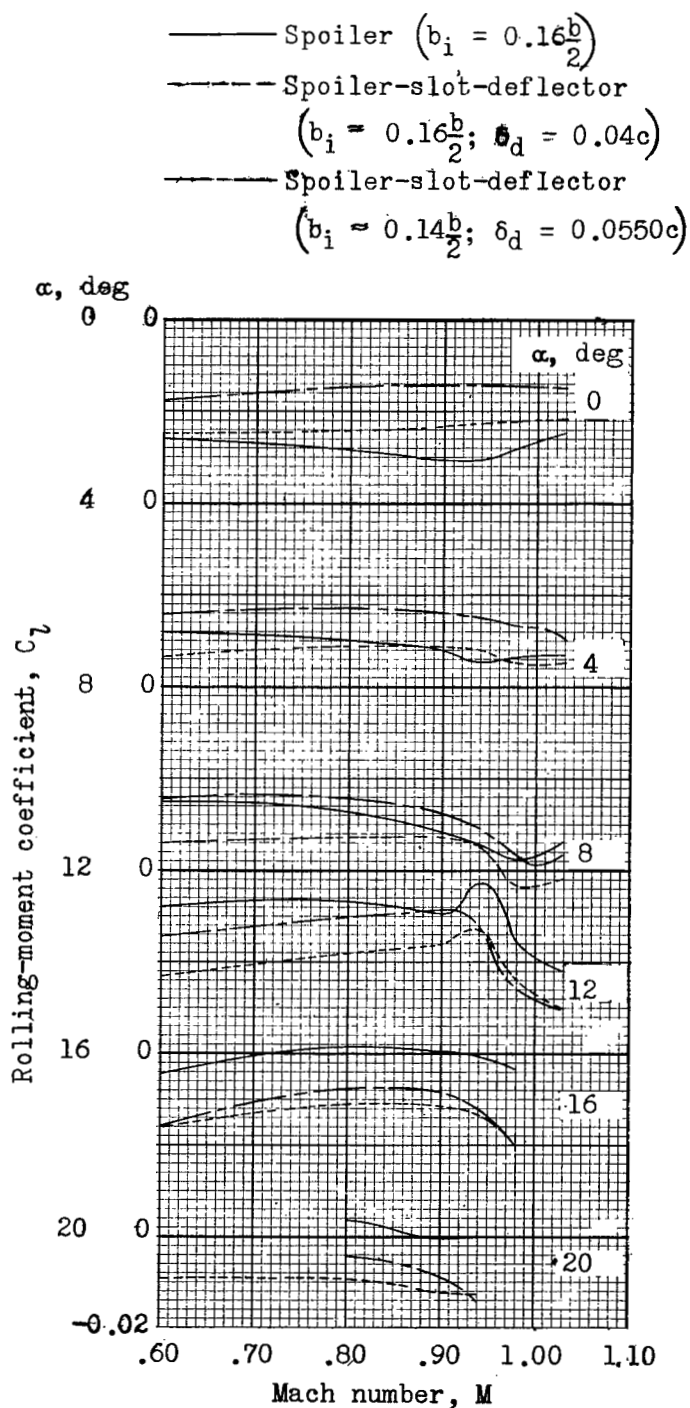


Figure 12.- Effect of Mach number on the rolling-moment coefficient of several spoiler configurations.

NASA Technical Library



3 1176 01437 2347

**CONFIDENTIAL**